

**TRACE ELEMENT ANALYSIS OF ENVIRONMENTAL AND
BIOLOGICAL SAMPLES USING TOTAL REFLECTION X-RAY
FLUORESCENCE (TXRF)**

THIS THESIS HAS BEEN ACCEPTED FOR
THE DEGREE OF **M.Sc** 1998
AND A COPY MAY BE DEPOSITED IN THE
UNIVERSITY LIBRARY.

KIPKIRUI ARAP KORIR

388450

UNIVERSITY OF NAIROBI
LIBRARY
P. O. Box 30197
NAIROBI

**A THESIS SUBMITTED IN PART FULFILLMENT FOR THE DEGREE
OF MASTER OF SCIENCE IN THE UNIVERSITY
OF NAIROBI**

1998

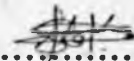
UNIVERSITY OF NAIROBI LIBRARY



0101644 3

Declaration:

This dissertation is a partial fulfillment for Master of Science degree at the University of Nairobi, and I hereby declare that it is my original work and has not been submitted elsewhere to the best of my knowledge.

Sign.......... Date: 31/12/, 1997

Kipkirui Arap Korir

This thesis has been submitted for examination with approval of the following University supervision:

Signature: ..... Date: 10/2/98.....

Mr. Maina, D. M.

Institute of Nuclear Science, University of Nairobi.

Signature: ..... Date: 10.2.98.....

Mr. Mangala, M. J.

Institute of Nuclear Science, University of Nairobi.

ACKNOWLEDGMENT

First and foremost, special thanks to my supervisors M. Maina and M. Mangala for their invaluable advice and guidance throughout the research, without which, this work could not have been accomplished.

I thank the University of Nairobi and the Institute of Nuclear Science for making this study possible by availing all the necessary facilities and the scholarship which enabled me to undertake the degree course. Dr P. Kregsamer for the installation of the TXRF Module, International Atomic Energy Agency (IAEA) and the Kenya National Council for Science and Technology (NCST) for their contributions in terms of facilities used. Prof. B. Holynska, an IAEA expert on Nuclear Techniques, for setting the pace in my research work.

I also wish to sincerely thank all those who contributed in whatever capacity to the successful completion of this work at the Institute of Nuclear Science and also for their co-operation. Among them are Dr. M. Kinyua (Director), Mr. M. Gatari (PCT), Mr. A. Matini (PT) and Mr. P. Ndwigah (ST).

Last but not least, I wish to sincerely thank my parents, Mr. and Mrs. Tergech, all brothers and sisters for their moral and material support during my formative years. My friends are also acknowledged for whatever contribution given to me, especially bro. Mwangi C.

| | |
|----------------|----|
| Introduction | 1 |
| Chapter I | 11 |
| Chapter II | 15 |
| Chapter III | 18 |
| Chapter IV | 21 |
| Chapter V | 24 |
| Chapter VI | 27 |
| Chapter VII | 30 |
| Chapter VIII | 33 |
| Chapter IX | 36 |
| Chapter X | 39 |
| Chapter XI | 42 |
| Chapter XII | 45 |
| Chapter XIII | 48 |
| Chapter XIV | 51 |
| Chapter XV | 54 |
| Chapter XVI | 57 |
| Chapter XVII | 60 |
| Chapter XVIII | 63 |
| Chapter XIX | 66 |
| Chapter XX | 69 |
| Chapter XXI | 72 |
| Chapter XXII | 75 |
| Chapter XXIII | 78 |
| Chapter XXIV | 81 |
| Chapter XXV | 84 |
| Chapter XXVI | 87 |
| Chapter XXVII | 90 |
| Chapter XXVIII | 93 |
| Chapter XXIX | 96 |
| Chapter XXX | 99 |

To EWM...

| | |
|--------------|----|
| CHAPTER I | |
| Introduction | |
| 1.1 | 1 |
| 1.2 | 2 |
| 1.3 | 3 |
| 1.4 | 4 |
| 1.5 | 5 |
| 1.6 | 6 |
| 1.7 | 7 |
| 1.8 | 8 |
| 1.9 | 9 |
| 1.10 | 10 |

| | |
|--------------|----|
| CHAPTER II | |
| Introduction | |
| 2.1 | 11 |
| 2.2 | 12 |
| 2.3 | 13 |
| 2.4 | 14 |
| 2.5 | 15 |
| 2.6 | 16 |
| 2.7 | 17 |
| 2.8 | 18 |
| 2.9 | 19 |
| 2.10 | 20 |

| | |
|--------------|----|
| CHAPTER III | |
| Introduction | |
| 3.1 | 21 |
| 3.2 | 22 |
| 3.3 | 23 |
| 3.4 | 24 |
| 3.5 | 25 |
| 3.6 | 26 |
| 3.7 | 27 |
| 3.8 | 28 |
| 3.9 | 29 |
| 3.10 | 30 |

| CONTENTS | page |
|---|-------------|
| Title | i |
| Declaration | ii |
| Acknowledgment | iii |
| Dedications | iv |
| Content | v |
| Figures and Tables | vii |
| Abstract | viii |
| CHAPTER ONE Introduction | |
| 1.1 Introduction | 1 |
| 1.2 The Need for Trace Element Studies of Environmental Samples | 5 |
| 1.3 Trace Element Intake in Human | 7 |
| 1.4 Project Objective | 9 |
| CHAPTER TWO Basic Principles of TXRF | |
| 2.1 X-ray Properties | 10 |
| 2.2 X-ray Interaction with Matter | 13 |
| 2.3 Total Reflection of X-rays | 16 |
| 2.4 Detection Efficiency | 25 |
| CHAPTER THREE TXRF Instrumentation | |
| 3.1 Experimental TXRF Spectroscopy and Optimisation | 27 |
| 3.2 Attachment of the Prototype TXRF module | 29 |
| 3.3 TXRF Module Optimisation | 32 |
| 3.4 Sample Preparation for TXRF Analysis | 33 |
| 3.5 TXRF Energy Spectrum | 37 |

CHAPTER FOUR

Experimental Procedures

| | |
|---|----|
| 4.1 Optimisation of TXRF Instrumentation | 38 |
| 4.2 Cleaning Procedures of Sample Containers, Sample Carriers and Teflon Bombs and Reproducibility | 40 |
| 4.3 Sampling and Sample Description | 43 |

CHAPTER FIVE

Results and Discussion

| | |
|---|----|
| 5.1 Optimisation Results | 46 |
| 5.2 Results of TXRF Analysis of Samples Prepared by Preconcentration Technique with NaDDTC | 52 |
| 5.3 Results of TXRF Analysis | 55 |

CHAPTER SIX

Conclusion and Recommendations

| | |
|---------------------|----|
| 6.1 Conclusion | 70 |
| 6.2 Recommendations | 72 |

| | |
|-------------------|-----------|
| REFERENCES | 73 |
|-------------------|-----------|

Figures

| | | |
|---------------|---|----|
| Figure 2.1 | Emission characteristic typical of molybdenum target operated at different voltages. | 12 |
| Figure 2.2. | Scattering of air in TXRF showing the characteristic peak of Argon. | 15 |
| Figure 2.3. | Excitation conditions of a sample under total reflection mode. | 16 |
| Figure 2.4. | Variation of reflectivity with incident angle for silicon. | 19 |
| Figure 2.5. | Variation of the line intensity (N_j) with sample thickness. | 22 |
| Figure 2.6. | Curves of detector efficiency versus energy for various window and detector thicknesses. | 26 |
| Figure 3.1. | Block diagram of a typical TXRF spectrometer | 27 |
| Figure 3.2. | Various parts of a basic Vienna prototype TXRF module | 28 |
| Figure 3.3. | Assembly of TXRF attachment module with the type-D housing | 30 |
| Figure 3.4. | Total reflection of low energy x-ray photons and absorption of the high energy non-reflected radiation. | 31 |
| Figure 3.5. | Aqueous sample preparation for TXRF analysis | 34 |
| Figure 3.6. | Solid sample preparation for TXRF analysis | 35 |
| Figure 5.1. | Variation of normalised background ratio of titanium, cobalt and strontium at different operating voltages, current set at 20 mA. | 46 |
| Figure 5.2. | Spectrum showing the cut off for high energy photons (keV) | 47 |
| Figure 5.3. | Variation of detection limits in pg with (+) and without (-) zirconium filter for molybdenum tube excitation source in TXRF | 48 |
| Figure 5.4. | Variation of detection limit (in pg) for a standard solution, on siliconized carrier (+) and non siliconized (-) (Time 1000s). | 49 |
| Figure 5.5. | Variation of strontium- $K\alpha$ net peak counts over a 70 day period for the control sample. | 50 |
| Figure 5.6. | Variation of relative elemental sensitivities with the corresponding atomic number for K-lines. | 51 |
| Figure 5.7. | Spectrum of a clean sample carrier. | 52 |
| Figure 5.8. | A spectrum of mineral water collected for 1000s using direct method of measurement. | 54 |
| Figure 5.9. | Spectrum of the same sample under similar conditions but pre-concentrated. | 54 |
| Figure 5.10. | Comparison of concentrations in mg/g for the unprocessed maize (raw) and the mean value for processed brands (sifted). | 59 |
| Figure 5.11. | Comparison of analysis results of concentration in $\mu\text{g/g}$ for normal and instant tea. | 60 |
| Figure 5.12. | Comparison of trace element intake in mg/day for food stuff in UK (1973) and average content in common raw food in Kenya. | 62 |
| Figure 5.13. | Typical spectrum of mineral water sample (G) with relatively high concentration of zinc elements. | 64 |
| Figure 5.14 | Relative concentration of trace elements in a running tap | 65 |
| Tables | | |
| Table 3.1 | Recent fields of TXRF application | 33 |
| Table 4.1 | Water samples and their description | 43 |
| Table 5.1 | Variation of analyte concentration (mg/ml) with time in seconds. | 48 |
| Table 5.2 | Comparison of results for direct and pre-concentrated sample preparation techniques in $\mu\text{g/g}$ for sample J. | 53 |
| Table 5.3 | Comparison of experimental and expected values of multi-elemental standards solutions (n=10). | 53 |
| Table 5.4 | Concentration variations in $\mu\text{g/ml}$ observed for a contaminated water sample. | 55 |
| Table 5.5 | Comparison of experimental and certified values in $\mu\text{g/g}$ for lyophilised Pig Kidney (BCR No. 186). (n=3) | 56 |
| Table 5.6 | Comparison of experimental and certified values of concentration in $\mu\text{g/g}$ for Chinese human hair | 56 |
| Table 5.7 | Comparison of experimental and certified concentration values in $\mu\text{g/g}$ of concentration for rye flour | 56 |
| Table 5.8 | Comparison of experimental and certified values in $\mu\text{g/g}$ for 'rice-unpolished' | 57 |
| Table 5.9 | Comparison of experimental and certified values of concentration in $\mu\text{g/g}$ for Japanese tea | 57 |
| Table 5.10 | Comparison of experimental and certified concentration values in $\mu\text{g/g}$ for kale reference standard | 57 |
| Table 5.11 | Results of analysis for three brands of processed maize flour with fresh maize in $\mu\text{g/g}$ after sample digestion. | 59 |
| Table 5.12 | Concentration levels of trace elements in $\mu\text{g/g}$ of instant and normal tea brands | 60 |
| Table 5.13 | Concentration levels in $\mu\text{g/g}$ of elements in various kale samples unless otherwise indicated | 61 |
| Table 5.14 | Analysis results for different water samples. | 63 |
| Table 5.15 | Comparison of experimental and predetermined values of potassium (K) and calcium (Ca) in $\mu\text{g/ml}$ for some samples. | 64 |
| Table 5.16 | Component loading of elements by some factors in maize samples and their contribution to the total variance. | 66 |
| Table 5.17 | Component loading of elements by some factors in tea samples and their contribution to the total explained variance. | 67 |
| Table 5.18 | Component loading of elements with sign. factors in kale sample and the factor contribution to the total explained variance. | 67 |
| Table 5.19 | Component loading of elements with significant factors in water samples. | 68 |

Abstract

Optimisation of the Total Reflection X-ray fluorescence spectrometer (TXRF) used in this work was accomplished by instrumental adjustments of relevant parameters, sample preparation and appropriate choice of excitation conditions. The TXRF module used was optimised for Mo x-ray tube at 40 kV and the Bremsstrahlung cut-off energy at 20.0 keV. Sample preparation method was chosen according to the nature and origin of the sample. Sample excitation efficiency depended largely on the homogeneity of the sample material on the carrier surface and the x-ray tube operating conditions. Sample preparation by preconcentration technique improved the detection limits of certain elements by a factor of over 50, in comparison to direct analysis method in which homogeneity and controlled spreading of the sample on the carrier surface rarely exceed a factor of two. In this study, spreading of 10 µl sample was limited to 5-6 mm diameter by completely drying the quartz sample carrier in a low pressure (350 mbars) oven at temperature of 70⁰ C for 10 hours.

Trace element analysis of various water samples that are sold in Nairobi as mineral drinking water and tap water was done to assess the environmental pollution from heavy metal contamination. For most samples analysed, the levels of potassium (K) ranged from detection limit (0.2 µg/ml) to 28.9 µg/ml, calcium (Ca) 2.2 to 120 µg/ml, titanium (Ti) detection limit (11 µg/l) to 60 µg/l, manganese (Mn) detection limit (8 µg/l) to 670 µg/l, iron (Fe) 31 to 540 µg/l, zinc (Zn) detection limit (8µg/l) to 4730 µg/l, bromine (Br) detection limit (8 µg/l) to 248 µg/l, rubidium (Rb) detection limit (10 µg/l) to 40 µg/l, and strontium (Sr) detection limit (8 µg/l) to 1000 µg/l. The experimental concentration values for potassium (K) and calcium (Ca) for most of the samples were in agreement to predetermined values (label). In general, most of the local mineral water samples contained higher levels of trace elements compared to the imported brands. Concentration levels of iron in 50 % of the imported, and 80 % of the local samples exceed the WHO maximum limits. Principal Component Analysis of the results for water samples revealed three factors of pollution sources. The highest component loading clustering include rubidium, strontium and calcium in the first eigenvalue; titanium, iron, bromine and zinc, in the second; zinc, manganese and potassium in the third. The percentage of total variance explained by the component was 31.4 %, 27.3 %, and 14.8% respectively.

For biological samples, three local food samples consumed by most Kenyans, and some certified reference materials were analysed. The samples were: cereal based; raw maize (*Zea mays*) and processed flour ; vegetable based; kale (*Brassica oleracea*) or locally referred to as *sukuma wiki*, and beverage based; instant and cured tea leaves (*Camelia sinensis*). The cereal based samples contain low levels of trace element compared to vegetable samples. The distributions of trace elements in these samples, to a large extent, are influenced by the type of

the food sample or environmental factors. Trace element intake in the Kenyan diets heavily relies on the consumption of kale that has significant proportion of strontium (107 ± 59) $\mu\text{g/g}$ and rubidium (89 ± 25) $\mu\text{g/g}$, tea leaves with manganese (1060 ± 169) $\mu\text{g/g}$ and rubidium (116 ± 26) $\mu\text{g/g}$. Consumption of maize meal contributes largely to Fe (27 ± 9) $\mu\text{g/g}$ intake given that it is the stable diet. The study also indicated that the concentration levels of the elements in the food stuff is modified by processing methods. Principal Component Analyses on the maize sample results indicated, 64 % of the observed total elemental concentration variance, was explained by a single factor while for kale and tea samples, the most significant factor explained only 45% and 42 % respectively.

CHAPTER ONE

INTRODUCTION

1.1 Introduction

Energy dispersive x-ray fluorescence analysis (EDXRF) method is an accepted analytical tool for elemental analysis of various samples. The technique depends on the emission of the characteristic radiation in the 1-60 keV energy range, following excitation of atomic electrons by an external energy source (Bertin, 1975). The elements that can be detected with standard detectors such as Si(Li), Ge(Li) and HpGe types range from atomic number 11 (sodium) upwards.

The information content of an energy dispersive x-ray spectrum is among the highest that one can obtain in a single measurement. The position and intensity of the spectral peaks provide qualitative and quantitative information; where the intensity of the spectral background may be used effectively to provide information concerning the bulk composition of the sample matrix. Total X-ray Reflection Fluorescence (TXRF) analytical technique is a special variant of energy dispersive x-ray fluorescence spectroscopy suited for elemental analysis of minute samples, especially those prepared on an optically flat surface and excited under total reflection conditions. Aiginger and Wobrauschek (1974).

Total reflection of x-rays was first described by Compton (1923) in the early 1920's when he demonstrated experimentally that x-ray could be reflected through angles of several milliradians by means of polished silver or glass mirrors. The utilisation of the total reflection of x-ray for analytical purposes was proposed by Yoneda and Horiuchi (1971). With the realisation that total reflection spectra is sensitive to surface roughness (Parratt, 1954) and that a mirror in the total reflection mode acts like a low pass filter (Nakana, *et al.*, 1978), the potential utility of the technique in routine analyses was born. Instrumental design for total x-ray reflection fluorescence progressed quickly after construction of the first basic TXRF unit by Aiginger and Wobrauschek (1974). Knoth and Schwenke (1978) pioneered the introduction of new instrumental design with automated sample changer. Modern versions of the TXRF units combine several mirrors to effect multiple reflection,

resulting in drastic reduction in spectral background and superior detection limits for most elements of interest (Schwenke and Knoth, 1991).

Special window materials that can withstand several atmospheres of pressure are currently replacing the detector beryllium window. By replacing the beryllium window of the detector with a thin carbon foil and performing all the measurements in vacuum, Streltsov *et al.*, (1993) extended the application of the TXRF technique to determine oxygen in various compounds. Because of the transmission properties of these window materials, the measurement of elements from boron ($Z=5$) is possible (Wobruschek *et al.*, 1991).

Radionuclides and x-ray tubes are often used as excitation sources in conventional x-ray fluorescence analysis. TXRF analysis requires an intense, collimated primary beam achievable mainly with x-ray tubes for sample excitation. A fine beam x-ray tube is preferable to provide a high x-ray flux on the thin sample film (Wobruschek, 1989). For low atomic (Z) element detection, the choice of the anode material, the angles of the incident electrons and of the emitted photons are of importance. Synchrotron radiation has recently provided superior results (Wobruschek, 1995), unfortunately it is expensive for most research applications. Synchrotron radiation excitation offers better results in comparison to x-ray tubes for sample excitation due to the high beam intensity, quasi-monochromatic nature and inherent collimated beam. In earlier studies, synchrotron radiation was applied in the TXRF excitation mode to the analysis of surface contamination in silicon wafers, with detection limits better than 1 ppb for metal ions deposited on the polished wafers after a counting time of 100 seconds (Atsuo, *et al.*, 1986). Third generation of dedicated synchrotrons could offer low detection limits in the attogram regime (10^{-15} g), (Wobruschek, 1995).

The TXRF module is a special equipment attached to an x-ray tube for total x-ray reflection analysis. The collimated primary beam of x-rays from the tube impinges on the surface of the sample carrier at angles of only few minutes of arc; below the critical angle for total reflection (Aiginger and Wobruschek, 1974). This physical phenomenon of total reflection of x-rays is because refractive index of x-rays in the quartz is slightly smaller than one. consequently, only a small part of the primary beam penetrates the carrier surface and has virtually no interaction with the sample carrier. This results in the observed low level of

scattered radiation and a substantial improvement in the signal to background ratio leading to superior detection limits for most elements of interest.

The most prominent features in the TXRF spectra are the characteristic x-ray fluorescence peaks originating from the thin sample, the sample carrier and argon peak from air. The background is caused incomplete charge collection in the detector and by scattering of the exciting radiation which results in very broad Compton peaks. Scattering of the 'white' spectrum or the continuous spectrum from the tube is also observed as background.

The problem in detecting elements at the nanogram or sub-ppb level is basically one of being able to obtain a signal that can be clearly distinguished from the background. Typically, the low detection limit (LLD) is specified by equation 1.1 (Wobruschek and Aiginger, 1975),

$$LLD = \frac{3}{s} \sqrt{\frac{I_B}{t}} \text{----- (1.1)}$$

Where

- s = elemental sensitivity in counts per second (cps) per unit mass,
- I_B = background intensity in cps,
- t = counting live time in seconds

A typical TXRF spectrum can have overlaps of spectral lines of various elements. As a result computer based spectrum analyses have become necessary. The method of iterative least squares analysis based on non-linear least-squares optimisation algorithm of Marquardt (1963) adopted in AXIL, QXAS software package (Kregsamer, 1995) is suitable for spectrum deconvolution. This method requires a systematic and accurate description of all the spectral features including energy calibration of the spectrometer and utilises a suitable fitting function. The model consists of essentially two cumulative portions, the background and the characteristic x-ray photopeak spectrum function. The background function is build up of different components, which depend on the excitation mode of the sample (Van Espen *et al*, 1977). For total reflection geometry a mathematical background model of exponential function of order five or six is used.

$$F_{B(i)} = \sum_{k=1}^i a_k (E_i - E_0)^k + b_0 e^{[b_1(E_i - E_0) + b_2(E_i - E_0)^2 + \dots + b_i(E_i - E_0)^i]} \quad \text{--- (1.2)}$$

Where E = energy, E₀ = suitable reference energy

This equation can be used to describe the entire spectrum. This function is non-linear in the parameters b₁,....., b_i.

Very little sample material in liquid form (1-10 µl) or as a fine suspension are required for trace element analysis using TXRF. The sample aliquot is normally deposited in the middle of a polished plane surface of a suitable substrate, usually a disk shaped quartz reflector (*Suprasil*) of diameter of 30 mm. The characteristic x-ray fluorescence radiation emitted from the small sample is collected by large solid angle detector positioned ~5 mm from the sample. Typically, the detection limits are in the nanogram range for most environmental and biological samples. For aqueous solutions, concentration in the ng/g (ppb) range is obtained without complicated sample preparation procedures. Many samples presented for TXRF analysis are in aqueous solutions or can be converted into that form by dissolution. Acidic dissolution at 180 °C and high pressure is an effective method for sample decomposition. Sample preparation techniques in TXRF have been extensively developed in recent years and successfully applied for trace analysis at picogram amounts of elements in various kinds of materials (Bohlen *et al.*, 1995; Pelpenik, *et al.*, 1993; Ojeda, *et al.*, 1993; Michaelis and Prange, 1988; Leland, 1987; Prange, *et al.*, 1985). If the sample cannot be prepared in this way, scattering can be suppressed by excitation with linear polarized beam and the appropriate x-y-z geometry of beam-sample-detector positions as presented by Wobrauschek (1995) using linear polarized synchrotron radiation.

Currently, the ranges of application of TXRF is wide and covers estuarine and marine water quality management studies, research in air pollution studies, mineralogical investigations, chemical oceanography, and medicine. Accordingly, numerous matrices have been handled and several sample preparation techniques adopted to TXRF analysis (Prange, 1989). With the computerisation of most of the core areas of the TXRF analysis, a lot of precious time and money can be saved in routine analysis of bulk samples.

1.2 The Need for Trace Element Studies of Biological and Environmental Samples

The process of dispersion of trace elements in the biosphere affects the whole ecosystem since elements dispersed in the atmosphere do not remain at a point as permanent contaminants, but are transported and eventually deposited in the ocean or on land. The subject of atmospheric pollution and its consequences on human health has received a great deal of attention since World War II (Purves, 1977; Junge, 1963; Magil, *et al.*, 1956). The atmosphere is considered mainly as a possible route for the contamination of the hydrosphere and the exposed surface soil. Several elements from industrial activities find their way in large quantities into the ocean, but so great is the total volume of water involved that the ecological consequences of such additions are largely restricted to situation where dispersion is delayed or restricted (Purves, 1977).

Presently, most trace-element pollution problems involve metals, but problems can arise also with non-metals like arsenic and boron. When a potential toxic element is absorbed by a living organism at abnormally high concentration, it may cause structural damage or enter cells and inhibit enzyme activities to such an extent that normal cell functioning is impaired (Mertz, 1979). Every element of the periodic table will produce some detrimental effect on man if the level of exposure is sufficiently abnormal. Although it is impossible to quantify the hazards and other deleterious effects associated with the exposure to trace elements, some elements such as lead, mercury and cadmium, present a greater health risk than others (Mertz, 1979). Other elements that are of environmental concern are: chromium, copper, fluorine, molybdenum, nickel and zinc. Less severe health effects are occasionally encountered with antimony, beryllium, selenium, silver and thallium, although dispersion of these elements in the biosphere is generally low.

Rainwater for example, has proved to be an exceptional form of transport for trace element from the atmosphere to terrestrial and aquatic environments. Besides acid rains, many heavy metals contribute to the hazards and destruction of forests, lakes and coastal waters, not to mention the adverse effects on the aquatic life (Jackella, *et al.*, 1984; Numberg, *et al.*, 1982). Studies of trace elements in some environment and biological samples were neglected in the past largely due to problems of sample contamination and inaccurate analysis at the low

levels involved (The National Research Council, 1977). These problems became even more severe as attempts were made to distinguish very small variation in some analytes in the samples. Usually, the elemental concentration levels are normally in the $\mu\text{g/l}$ to ng/l range and the analytical procedures applied are usually based on inverse voltammetry and atomic absorption spectrometry as analytical techniques (Pinta, 1978). These techniques allow either single element determination or selective determination of not more than three elements simultaneously. Various attempts in the past based on these techniques to study trace elements in environmental and biological samples are mentioned in some references (Michaelis, 1983; Iyengar and Sansoni, 1980; Iyengar and Sansoni, 1978). More recently, multi-elements trace studies has been performed quite effectively at low levels of concentration using TXRF analytical technique (Prange, *et al.*, 1985; Bohlen *et al.*, 1987; Bohlen *et al.*, 1987; Bohlen *et al.*, 1988; Pelpenik, *et al.*, 1993; Ojeda, *et al.*, 1993).

1.3 Trace Elements Intake in Human

There is increasing need for up-to-date and accurate data on trace element contents in food samples. This is useful in designing therapeutic diets and research on human trace element deficiencies and overexposure (The National Research Council, 1977). Because of the interactive nature of some elements, multi-disciplinary elemental studies are essential to provide data on the patterns and causal relationship between trace element intake and health-disease conditions (Pooreboom, 1985).

The task of determining trace element intake in man, including determination of the normal range of dietary intake can be simplified by the use of reliable, simultaneous multi-element analytical techniques. Trace element content of local indigenous diets and mineral water in Kenya is insufficient and lacking. It was therefore the aim of this study to begin tackling this problem by analysing some local foodstuffs. The accrued data would help in the assessing the nutritional values of some local food products.

The major source of most elements for the body is diet. As such it is important to determine the levels of elements in prepared food in addition to that in raw food samples. In food preparation, considerable elemental changes takes place. For example, loss from cooking, addition from utensils, and food additives (table salt, seasoning). In addition, the selection of some parts of the raw food products, chemistry of the elements and other physiological processes, does contribute to the overall effects and the trace element content (Davies and Nightingale, 1975). Consequently, the differential availability of trace elements in food samples has limited use for determining the nutritional requirements of most diets (Hambidge, 1974).

Developments in agriculture and technology also does affect the trace element content of foods (Davies and Nightingale, 1975). For example, the introduction of new varieties of plants, the use of agricultural chemicals and other new techniques designed to increase food production and yields are likely to affect the composition of basic food samples. Consequently, the major factors which influence the amount of trace elements in food consumed are (Davies and Nightingale, 1975): (i) inherent characteristics of plants as dictated

by species; (ii) environmental conditions affecting plants such as soil composition and pH; (iii) methods for handling, processing, maturity and choice of plant portion harvested.

Water constitutes the next most important source of elements to man. Its quality is particularly of paramount importance to all people (Hamilton, 1974). In most instances, the levels of elements in potable water tend to be low but a water factor yet unidentified, is suspected in relation to the incidence of cardiovascular diseases attributed to soft water Masironi (1972). According to Masironi, hard water maybe considered to be beneficial and soft water harmful. Guidelines for acceptable limits of trace elements in drinking water are prepared under the auspices of the World Health Organisation among other concerned organisations (The National Research Council, 1977).

Water supplied by commercial undertakings if following strict quality regulations, seldom would they give rise to concern for health. The same may not be true for water from natural wells and surface waters. However, water sampled from domestic taps can be contaminated as a result of contact with plumbing materials or the random presence of suspended solids that are present in most natural water systems (Kinyua, 1982). The trace element content of the water consumed by many groups of people in remote parts of Kenya has not been determined. For generations, they have been drawing their water from natural springs and taking it without any treatment. Other people rely heavily on rain water that is normally collected from house roof tops. Most modern houses use corrugated iron sheets for roofing and in many instances, the roofs are coated with different sorts of paints most of which contain zinc or lead. Over exposure to some of these elements can be hazardous.

The existing data on trace element levels in most samples mentioned before were limited through the use older analytical techniques. For example, most analyses for levels of elements in water were accomplished only after the use of some form of pre-enrichment technique, which often was a source of contamination (Kinyua, 1982; Hamilton, 1974). Great progresses achieved recently in terms of analytical tools and methods for trace element analysis have enabled reliable analysis for the essential trace elements in foods. However, more research is needed to establish the levels in the indigenous foodstuffs, as a function of geographical area and the feeding habits.

1.4 Project Objectives

The objectives of this research (study) were:

- (i) Optimisation of TXRF spectrometer with a Vienna TXRF prototype module.
- (ii) Determine suitable methods for sample preparations for determination of trace element in both environmental and biological samples using TXRF method.
- (iii) Quality control of some certified material of biological origin so as to assess the suitability of the technique for analyses of 'unknown' samples of similar matrices.
- (iv) To determine the distribution and concentration of trace elements, in mineral water samples and the possible extent of contamination from heavy metals.
- (v) Determine the levels of trace elements in local food samples (maize, kale and tea).

CHAPTER TWO

BASIC PRINCIPLES OF TXRF

2.1 Properties of X-ray

X-rays are electromagnetic radiation of wavelength $\sim 10^{-5}$ m to $\sim 10^{-15}$ m produced mainly as a result of velocity change of charged particles in an electromagnetic field, and during electron transitions in the inner shells of atoms. They form a part of the broad electromagnetic radiation spectrum. The very short wavelength nature of the radiation makes its quantum nature more prominent in most interactions with matter. X-ray is treated in quantum theory as consisting of particles known as photons.

X-ray radiation is emitted as continuous spectra or as line spectra characteristic of the emitting element. They undergo photoelectric absorption in matter and thereby produce characteristic spectra. In TXRF, both characteristic emission and continuous spectra from x-ray tubes are responsible for the emission spectra of a sample. The ability of the energetic x-ray photons to induce characteristic x-ray line spectra in sample materials is one of the most important property and basis of x-ray emission spectroscopy.

2.1.1 Continuous Emission Spectra (Bremsstrahlung)

Emission of x-rays with smooth, continuous function of energy is called the continuous emission spectra or Bremsstrahlung, (Figure 2.1). The continuum is produced as a result of progressive deceleration of high energy electrons impinging upon the x-ray tube anode. The shortest wavelength λ_{\min} of x-ray is given by the expression:

$$\lambda_{\min} = \frac{12.396}{V} \text{-----} (2.1)$$

Where V is the acceleration potential in kV.

The continuum profile is approximated by the Kramers formula (Bertin, 1973)

$$I_{\lambda} = kiZ \left(\frac{1}{\lambda_{min}} - \frac{1}{\lambda} \right) \frac{1}{\lambda^2} \text{-----(2.2)}$$

Where,

- k - is a constant;
- I_{λ} - is the intensity of wavelength λ ;
- λ_{min} - short wavelength limit;
- i - x-ray tube current;
- Z - the atomic number of the target.

The effect of the tube target atomic number **Z**, current **I** and the potential **V** on the continuum intensity I_{int} is best expressed by the Beatty formula (Williams, 1987),

$$I_{int} = 1.4 \times 10^{-9} ZiV^2 \text{-----(2.3)}$$

Where I_{int} describes the total power in watts; the maximum beam intensity corresponds to $\sim 1.5\lambda_{min}$ from equation 2.2.

2.1.2 Excitation of Characteristic Radiation

When an energetic photon or electron ejects an electron in the K, L or M shells of an atom, a vacancy is created. For the atom to gain stability, an electron from a higher level moves to occupy the vacancy. This can result in the emission of characteristic x-ray photon. According to selection rules of quantum theory, only certain transitions are 'permitted'. The characteristic x-ray emission spectra of an x-ray tube consist of discrete energies characteristic of the emitting target elements (Figure 2.1). The uniqueness of characteristic emission radiation form the basis of qualitative analysis in x-ray fluorescence spectrometry. Besides x-ray emission, other competing processes such as Auger and Compton recoil electrons occur within the sample (Bertin, 1975).

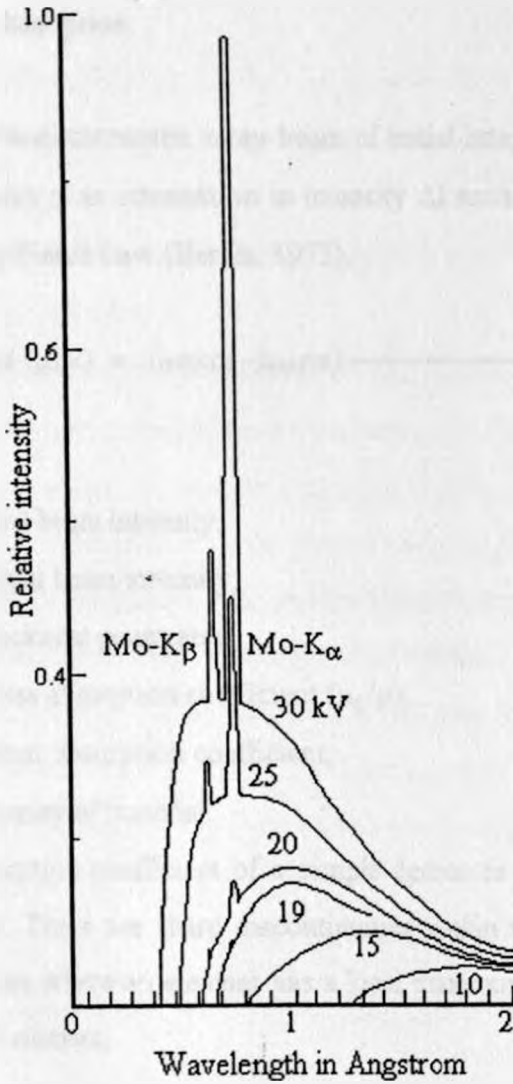


Figure 2.1 Emission characteristic typical of molybdenum target operated at different voltages, (Bertin, 1973).

The energy intensities of the x-ray spectrum produced as primary beam by an x-ray tube, varies with the applied potential according to this expression (Bertin, 1973),

$$I \propto i (V - V_k)^{-1.7} \text{-----(2.4)}$$

Where

i = x-ray tube current (mA);

V = x-ray tube potential (kV);

V_k = excitation potential (kV).

2.2 X-ray Interaction with Matter

2.2.1 X-ray Absorption

Considering a monochromatic x-ray beam of initial intensity I_0 , traversing through a thin layer of width Δx there is an attenuation in intensity ΔI such that, the final transmitted intensity is given by Bragg-Pierce Law (Bertin, 1973),

$$I = I_0 \exp(-\mu_L x) = I_0 \exp(-\mu_M \rho x) \text{-----(2.5)}$$

Where,

- I = final beam intensity;
- I_0 = initial beam intensity;
- x = thickness penetrated;
- μ_M = mass absorption coefficient (μ_L/ρ);
- μ_L = linear absorption coefficient;
- ρ = density of material.

The mass absorption coefficient of a sample decreases steadily with increasing energy of the incident x-rays. There are sharp discontinuities within the energy-absorption spectrum at the absorption edges where an element has a local maximum, corresponding to the characteristic energies of the element.

2.2.2 X-ray Scattering

When x-ray photons impinge on an atom, the photons may interact with electrons of the target element resulting in scatter of the x-ray photons. Scattered x-ray is one of the sources of background obtained in TXRF spectrum. The inelastic scattered x-rays are mainly due to the process of interaction with the outer, weakly held electrons of the elements. There are two scattering processes, namely coherent and incoherent scatter (Johns, 1953). Coherent scattering is an elastic process whereby the initial x-ray photon does not lose part of its initial energy. Photons are scattered by bound electrons in a process where the atom is neither excited nor ionised. The scattering from different parts of the atomic cloud combine to

produce coherent scattering. Coherent scattering cross-section per unit solid angle is represented mathematically by (Johns, 1953),

$$\frac{\partial \sigma_{coh}}{\partial \Omega} = \frac{r_0}{2} (1 + \cos^2 \theta) [F(x, 2)]^2 \quad \text{----- (2.6)}$$

Where

r_0 = classical electron radius (equal to 2.82×10^{-13} cm);

θ = scattering angle;

$F(x, 2)$ = atomic form factor with $x = \sin(\theta/2)/\lambda$ and λ = wavelength.

The cross section varies according to the energy of the x-ray photon, and may be useful in describing the variations of coherent scattering with the energy of the x-ray photons in a beam of x-ray. Minimal scattering for low photon energies (<100 keV) is situated at solid angles subtended at 90° with respect to the photon beam direction. Excitation mode in total reflection x-ray fluorescence allows the solid angle to be subtended at close to 90° resulting in minimal scattering to the detector crystal. In inelastic collision, the x-ray photon may lose energy to the colliding electron causing it to be ejected from its orbit. The energy loss, assuming a collision with a classical free electron, observed due to the Compton scatter results in photon of energy given by (Williams, 1987);

$$E' = \frac{E}{1 + 0.00196E(1 - \cos \theta)} \text{ keV} \quad \text{----- (2.7)}$$

Where

E' = scattered radiation energy;

E = incident x-ray energy;

θ = angle between the scatter and incident x-ray beam.

For $\theta \cong 90^\circ$, the Compton energy peak is observed at approximately;

$$E' = \frac{E}{1 + 0.00196E} \text{ keV} \quad \text{----- (2.8)}$$

In terms of Compton scattering, cross-section per unit solid angle is given by

$$\frac{\partial \sigma}{\partial \Omega} = \frac{\partial \sigma_0}{\partial \Omega} \cdot F_{KN} \quad \text{-----(2.9)}$$

Where σ_0 is the classical Compton scattering cross-section defined as ,

$$\frac{\partial \sigma}{\partial \Omega} = \frac{r_0^2}{2} (1 + \cos^2 \theta) \cdot F_{KN} \quad \text{-----(2.10)}$$

Where F_{KN} is;

$$F_{KN} = \left\{ \frac{1}{1 + (1 - \cos \theta)} \right\}^2 \left\{ 1 + \frac{\alpha^2 (1 - \cos \theta)^2}{[1 + \alpha (1 - \cos \theta)] (1 - \cos^2 \theta)} \right\} \quad \text{(Klein - Nishina formula (Johns, 1953))}$$

Figure 2.2 represents a spectrum for scattered primary x-rays collected for 1000 seconds from molybdenum x-ray tube. The spectrum shows the Mo - K_α peak, its Compton peak and the Argon peak. The background contribution is due to scattering of the continuum.

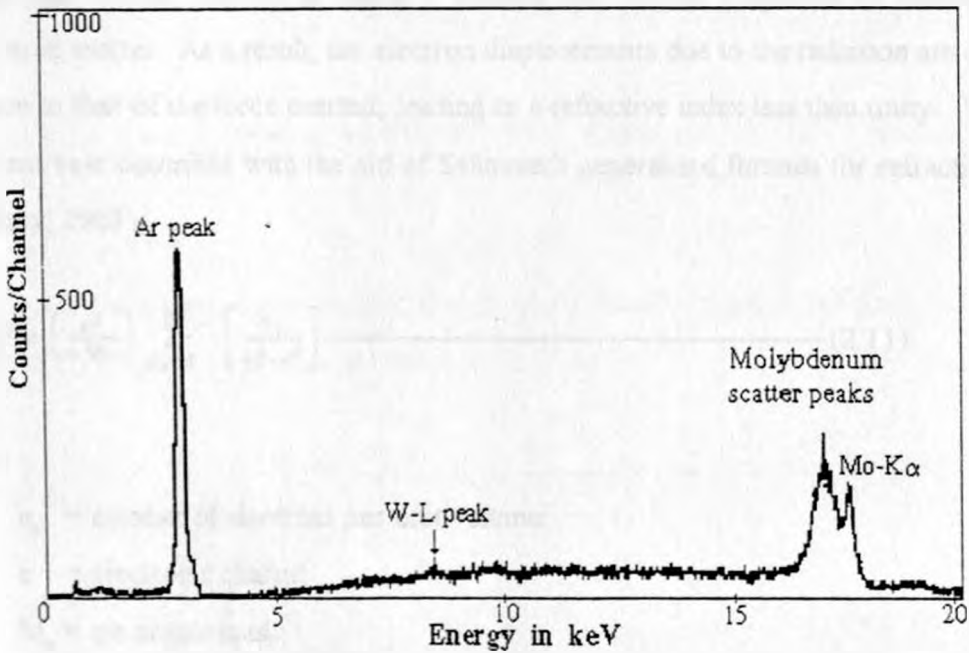


Figure 2.2 Scattering of air in TXRF showing the characteristic peak of Argon.

2.3 Total Reflection of X-rays

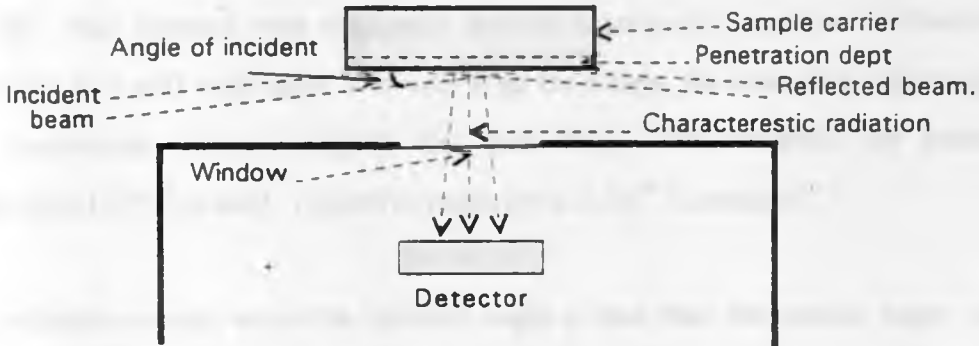


Figure 2.3 Excitation conditions of a sample under total reflection mode.

Total reflection of x-rays relies on the fact that the refractive index of x-rays in quartz is slightly less than unity (Parrat, 1954). The frequency of x-ray waves is so much greater than that of light waves, that in all cases it exceeds the natural frequency of vibration of the electrons in matter. As a result, the electron displacements due to the radiation are opposite in direction to that of the force exerted, leading to a refractive index less than unity. This results is perhaps best described with the aid of Sellmeier's generalised formula for refractive index η (Tolansky, 1963),

$$\eta^2 = \left(\frac{e^2}{\pi M_e} \right) \sum_{n_e=1}^N \left[\frac{n_e}{v_e^2 - v^2} \right] \text{-----} (2.11)$$

Where

- n_e = number of electrons per unit volume;
- e = electronic charge;
- M_e = electronic mass;
- N = number of different kinds of electron (different bound electrons);
- v_e = characteristic frequency of the electron;
- v = frequency of the incident light wave.

Clearly if $v > v_e$ then η is less than unity. Furthermore, if $v \gg v_e$ we have approximately,

$$\eta = 1 - \left(\frac{ne^2}{2\pi M_e v^2} \right) \text{-----(2.12)}$$

Although this formula was originally derived classically, quantum mechanics methods proved that it is still valid since v is very high for x-rays, the refractive indices given by the above expression are only slightly less than unity. For example, for quartz, when a wavelength of 0.7\AA is used, refractive index (η) $\cong 1-10^{-6}$ is obtained.

Total reflection occurs when the incident angle is less than the critical angle of reflection. This occur when the real part of the refractive index,

$$\eta = 1 - \delta - i\beta \text{----- (2.13)}$$

is less than one. β describes the attenuation of x-rays in matter given by,

$$\beta = \frac{\mu \lambda}{4\pi} \text{----- (2.14)}$$

Where μ is the linear absorption coefficient for the mirror and λ is the wavelength of incident radiation.

According to the classical dispersion theory, the variation of x-ray radiation energy in regions far from any absorption edges of the material is given by,

$$\delta = \frac{n_e e^2 \lambda^2}{2\pi M_e c^2} \text{----- (2.15)}$$

and,

$$n_e = \frac{N_A \rho Z}{A} \text{----- (2.16)}$$

- where, N_A = Avogadro's number;
- ρ = density of the material;
- Z = atomic number;
- A = atomic weight of the material.

In general, for total reflection of the incident beam of x-rays to occur, then Snell's law is applied,

$$\cos \Psi_c = 1 - \delta \text{ ----- (2.17)}$$

Where Ψ_c is the incident glancing angle at which the angle of refraction inside the mirror material is zero. For small angles, say in the order of a few milliradians, the equation above is approximated by,

$$\Psi_c = \sqrt{2\delta} \text{ ----- (2.18)}$$

By substituting equation (2.15) and (2.16) into (2.18) an expression for the critical angle expressed in terms of the wavelength and the physical properties of the reflector material may be obtained as,

$$\Psi_c = \left[N_A \rho \frac{Z}{A} e^2 \frac{\lambda^2}{\pi M_e c^2} \right]^{\frac{1}{2}} \text{ ----- (2.19)}$$

After substituting for Avogadro's constant, the electronic mass, electronic charge and the velocity of light, a simple expression for the critical angle as a function of the incident wavelength is obtained,

$$\Psi_c = \left(5.4 \times 10^{10} \frac{Z}{A} \rho \lambda^2 \right)^{\frac{1}{2}} \text{ ----- (2.20)}$$

Where

Ψ_c = angle in mrad;

ρ = density of quartz (2.5 gcm⁻³);

λ = wavelength of the radiation.

For quartz crystal material, the critical angle for total reflection is,

$$\Psi_c = \frac{32.2}{E} \text{ ----- (2.21)}$$

Where E is the energy reflection cut off in keV. X-ray photons of energies greater than E are refracted and those below are reflected. With molybdenum target whose characteristic radiation energies $K_{\alpha} = 17.5$ keV and $K_{\beta} = 19.6$, a cut-off energy at 20 keV is convenient. Using equation 2.21, $\Psi_c \cong 1.6$ mrad for a zinc sulphide screen at a distance of 1m away. Equation 2.21 also gives the upper bound limit for the range of angles where total reflection occurs for the incident photon energy from the source. Due to the abrupt drop in the reflected beam intensity at the critical angle, the cut-off energy acts as a low pass filter (Parratt, 1954; Nakana, *et al.*, 1978).

The reflectivity R of a material, in terms of critical angle, attenuation, absorption of the material and Fresnel coefficient for reflection (h) is given as (Parratt, 1954);

$$R = \frac{h - (\Psi/\Psi_c) \sqrt{2(h-1)}}{h + (\Psi/\Psi_c) \sqrt{2(h-1)}} \text{-----(2.22)}$$

where,

$$h = (\Psi/\Psi_c)^2 + \left\{ [(\Psi/\Psi_c)^2 - 1]^2 + (\beta/\delta)^2 \right\}^{\frac{1}{2}}$$

and other terms are as defined earlier.

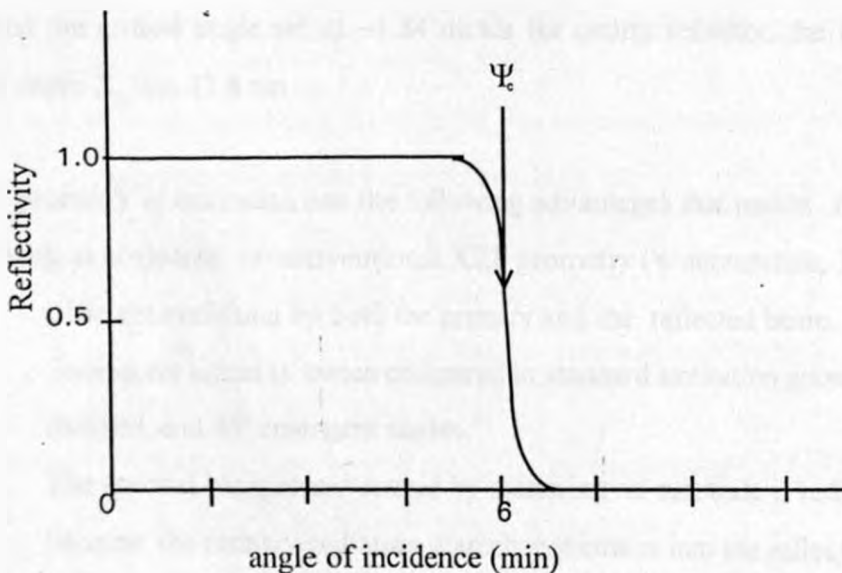


Figure 2.4. Variation of reflectivity with incident angle for silicon.

A plot of the variation of the reflectivity for silicon as a function of incident angles for silicon is given in figure 2.4 (Schwenke and Knoth, 1982). The curve shows that the reflectivity of

silicon drops abruptly after the critical angle of reflection is exceeded making it an ideal reflector. The reflectivity is maximum for angles less than the critical angle but decays abruptly to near zero immediately the ratio of the incident angle to critical angle passes one (Parratt, 1954). This property makes silicon a better reflector in comparison with other substitutes such as Plexiglass, quartz, germanium and glassy carbon all of which are the best choices for sample reflector materials, because they are reasonably inert to acid attacks. The choice of these materials as mirrors are also influenced by the fact that they are relatively free from contamination as they can be produced to very high degree of purity. They can be machined and polished to a high degree of flatness and smoothness. In TXRF setup, the quartz sample carrier has a dual function of being a reflector and sample carrier.

An important feature associated with the reflection is the penetration depth X_p . This is the distance in the sample carrier at which the intensity of the incident radiation falls to 1/e of its original value and is given by,

$$X_p = \frac{\lambda}{4\pi \left[\left\{ (\psi^2 - \psi_c^2) + 4\beta^2 \right\} - (\psi^2 - \psi_c^2) \right]^{1/2}} \quad (2.23)$$

This relationship is significant in surface and depth studies (Knoth, *et al.*, 1989). The smaller the magnitude of penetration depth, the better is the reflector. For Mo- K_{α} (17.48keV) radiation and the critical angle set at ~1.84 mrad for quartz reflector, the typical value of penetration depth X_p is \cong 73.8 nm.

The TXRF geometry of excitation has the following advantages that makes it more suited to analytical work as compared to conventional XRF geometry (Wobrauschek, 1995):-

- i. Efficient excitation by both the primary and the reflected beam. The fluorescent signal is twice compared to standard excitation geometry at 45° incident, and 45° emergent angles.
- ii. The spectral background caused by scattering on substrate is reduced because the primary radiation scarcely penetrates into the reflector substrate (high reflectivity, low transmission of the substrate material).
- iii. The scatter contribution from the sample itself is a minimum because of the 90° condition between incident and scattered radiation towards the detector.

- iv. The detector is mounted very close to the sample on the reflector surface resulting in a large detector solid angle.
- v. Only small volumes (1-10 μl) of liquid samples of small amounts are required. The samples are prepared in such a way that thin film approximation is applicable. Therefore no absorption occurs and a linear correlation between intensity and concentration of the elements is valid.

In TXRF excitation, the peak signal to background ratio is increased by more than 3 or so orders of magnitude as compared to conventional XRF method of sample excitation (Wobruschek, 1995). Improvement in the detection limits can be expected if the physical parameters influencing the minimum detection limits are optimised. From the expression of detection limit LLD, given in equation 1.1, the following experimental parameters (Wobruschek and Aiginger, 1975) determine the elemental sensitivity, s :

- i. The intensity of the primary excitation beam.
- ii. The distances, source to sample and sample to detector.
- iii. The detector active area.
- iv. The insertion devices in the primary beam path to modify the spectral distribution of the excitation radiation by lowering the background without necessarily reducing the primary intensity.

The spectral background intensity I_g depends upon:

- i. The primary intensity, its spectral energy distribution and the respective scattering cross-sections for the scatterers.
- ii. The sample mass distribution (for thin samples).
- iii. The geometric form and the material substrate, as well as the penetration depth of the primary radiation into the substrate and the reflection coefficient which is practically one.
- iv. Measurements done in air leads to unnecessary scatter of the radiation and also contribute to characteristic argon peaks.
- v. The actual adjusted angle of incidence.
- vi. Solid angle of the detector.

When a sample is excited by a nearly monochromatic primary beam, e.g. Mo-target K_{α} -lines, the intensity of the spectral line of an element j is given by (Klockenkamper and Bohlen, 1989).

$$N_j \approx c_j k_j \frac{1 - \exp(-\frac{\mu}{\rho} \rho t)}{(\mu/\rho) \rho} N_0 \quad \text{----- 2.24}$$

where

- N_j = net intensity of the element j line ;
- c_j = mass fraction or concentration of the analyte;
- k_j = proportionality factor for the analyte line;
- (μ/ρ) = mass absorption coefficient of the entire specimen;
- t = thickness of the specimen;
- N_0 = intensity of the incident monochromatic excitation x-ray beam.

A plot of line intensity N_j versus thickness t result in the following typical curve;

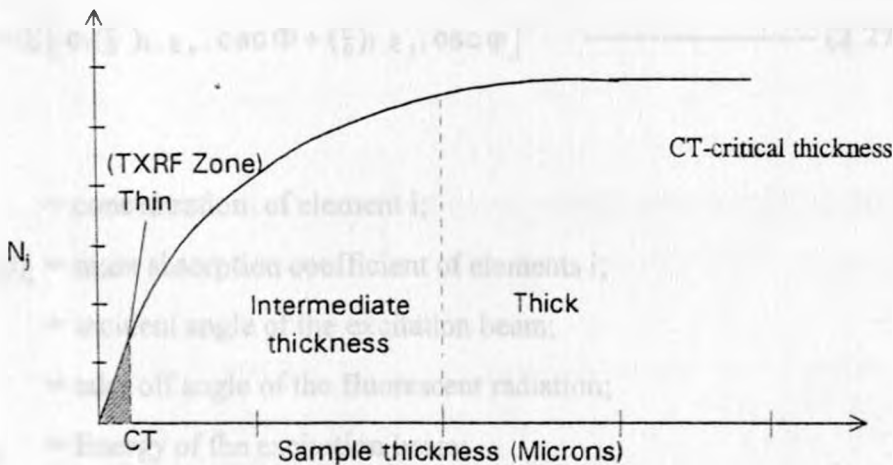


Figure 2.5 Variation of the line intensity (N_j) with sample thickness (Kregsamer, 1995).

Equation 2.24 is an approximation since the enhancement due to secondary (and tertiary) fluorescence is neglected. The equation appears to express proportionality between analyte line intensity and concentration, but these quantities are not proportional since the concentration c_j is also included in the (μ/ρ) quantity as shown by Figure 2.5 (Bertin, 1975). For 'infinitely' thin films, the analyte line intensity is directly proportional to the concentration c_j and to the thickness of the sample t , so equation 2.24 reduces to,

$$N_j = c_j K_j N_o t \text{ ----- (2.25)}$$

This relationship allows for evaluation of concentration of the element of interest. A criterion for a sample to be "infinitely" thin requires that the matrix effects be minimised. This can be achieved if the exponential term of equation 2.24 is relatively small. To deduce the critical thickness, (CT in Figure 2.5) of a sample with minimal matrix effects, a value of 0.1 is chosen (Bertin, 1975; Klockenkamper and Bohlen, 1989) as a close approximation such that deviation in the intensity N_j lies within 5 % i.e.

$$t \leq \frac{0.1}{(\mu/\rho) \rho} \text{ ----- (2.26)}$$

The mass absorption of the entire matrix is obviously composed of the coefficients of the various elements,

$$(\mu/\rho) = \sum \left[c_i \left(\frac{\mu}{\rho}\right)_{i, E_o} \cdot \text{csc } \Phi + \left(\frac{\mu}{\rho}\right)_{i, E_j} \cdot \text{csc } \phi \right] \text{ ----- (2.27)}$$

where,

- c_i = concentration of element i;
- $(\mu/\rho)_i$ = mass absorption coefficient of elements i;
- Φ = incident angle of the excitation beam;
- ϕ = take off angle of the fluorescent radiation;
- E_o = Energy of the excitation beam;
- E_j = Energy of the element j line;

The above expressions are true if the x-ray excitation beam is monochromatic and penetrates the sample only once. Experimentally, this is approximately realised in TXRF arrangement if (Klockenkamper and Bohlen, 1989):

- (i) The Mo -tube is operated at >30 kV, although the L-lines and the Bremsstrahlung continuum are also emitted, the K-peaks are by far the most intense lines.
- (ii) The experimental arrangement for total reflection shows that the second condition is fulfilled before the primary beam is totally reflected, thus the primary beam penetrates a flat, homogenous sample almost twice.

The sensitivity S_j of an element j is defined (Klockenkamper and Bohlen, 1989) with regard to its analyte line in the spectrum j as;

$$S_j = \frac{N_j}{C_j} \text{-----} (2.28)$$

where N_j is the line intensity given and C_j is the concentration. For a thin sample excited by a monochromatic excitation beam in total reflection condition, a factor 2 due to incident and reflected beams, is introduced such that (Klockenkamper and Bohlen, 1989);

$$S_j = 2K_j N_o t \text{-----} (2.29)$$

Where,

N_o = intensity of the excitation primary beam;

t = thin sample thickness;

and K_j represented by several factors such that,

$$S_j = 2g_L \omega_j \frac{r_j^{-1}}{r_j} (\mu/\rho)_{i, E_o} \cdot \rho \text{csc } \Phi \frac{\Omega}{4\pi} t N_o \text{-----} (2.30)$$

Where,

g_L = relative transition probability for the particular analyte line in its series;

ω_j = fluorescent yield of the analyte line;

r_j = jump ratio at the absorption edge;

$(\frac{\mu}{\rho})_{i, E_o}$ = mass absorption coefficient (photoelectric part) of the element for the excitation beam of energy E_o ;

ρ = density of the specimen;

Φ = incident angle of the excitation beam with the sample;

Ω = solid angle of the effective aperture of the detector;

If originally the thin sample had two elements i and s (introduced as internal standard with known concentration), then the two sensitivities can be evaluated and the constants eliminated resulting in a simple quantitative approach for determination of concentration of the unknown element i is given by;

$$C_i = \frac{N_i S_s}{N_s S_i} C_s \text{-----} (2.31)$$

where,

c_s = concentration of the internal standard element s ;

c_i = the unknown concentration value of element i ;

S_i / S_s = relative sensitivities; N_i / N_s = relative line intensity values.

By plotting a graph of relative sensitivities (S_i/S_s) versus the atomic number Z of the elements in multi-elemental standard solutions and performing a curve fitting, it is possible to determine the sensitivity of any other element through inter and extrapolation. The element chosen as the internal standard is one whose characteristic peak energy is within the region of interest and should be below the detection limit in the samples. Internal reference element is used in TXRF analysis because it minimise problems due to sample homogeneity and spreading on the carriers (Ninomiya, 1989).

2.4 Detection Efficiency

The detector efficiency ϵ of a Si(Li) detector is a function of energy to which it has been exposed. For low energy x-ray radiation there is a loss of efficiency due to attenuation of x-rays in the detector entrance window, dead layer and in the radiation air path. This problem affects the detection efficiency of mainly the low atomic number elements. At high energies the detector itself becomes transparent to photons, allowing the incident radiation to pass through the active volume without interaction, and capturing only part of the photon energy. (Klockenkamper and Bohlen, 1989). Curves showing the variation of detector efficiency with photon energy for different detector window thicknesses, are shown in figure 2.6.

The detector efficiency is described by the following expression (Klockenkamper and Bohlen, 1989);

$$\epsilon = \exp\left[-\left(\frac{\mu}{\rho}\right)_{Be} \rho_{Be} t_{Be} - \left(\frac{\mu}{\rho}\right)_{Au} \rho_{Au} t_{Au} - \left(\frac{\mu}{\rho}\right)_{Si} \rho_{Si} t_{Si}\right] \left\{ 1 - \exp\left[-\left(\frac{\mu}{\rho}\right)_{Si} \rho_{Si} d_{Si}^2\right] \right\} \quad (2.32)$$

where

t_{Be} , t_{Au} , t_{Si} = beryllium window, gold-film contact and silicon dead layer thicknesses respectively;

$(\mu/\rho)_{Be}$, $(\mu/\rho)_{Au}$, $(\mu/\rho)_{Si}$ = mass absorption coefficients of beryllium, gold and silicon respectively; d_{Si}^2 = silicon crystal thickness.

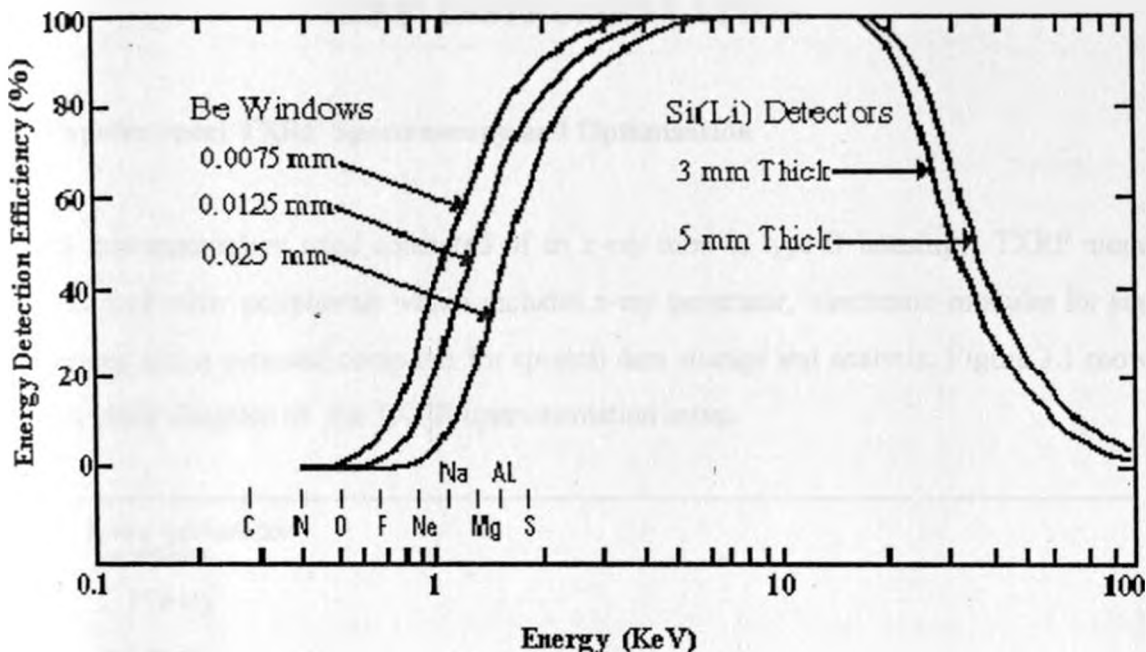


Figure 2.6 Curves of detector efficiency versus energy for various window and detector thicknesses (Canberra, 1993).

The absorption of x-rays by air on their path between the sample and the detector can be neglected for energies above 8 keV but increases strongly for lower energies (Canberra, 1993). The transmission is described by,

$$T = \exp [-(\mu/\rho)_a \rho_a d_a] \text{-----(2.33)}$$

where

$(\mu/\rho)_a$ = mass absorption coefficient of air;

ρ_a = air density, ($\rho_a = 0.0012 \text{ g/cm}^3$);

d_a = path distance ($d_a < 1.0 \text{ cm}$ for typical TXRF settings).

Transmission factor of low energy x-ray in air is low, hence molybdenum L lines are normally not observed in the spectrum with molybdenum excitation tubes. This factor is incorporated into equation 2.32 to get the ultimate detection efficiency of an analyte line.

CHAPTER THREE

TXRF INSTRUMENTATION

3.1 Experimental TXRF Spectroscopy and Optimisation

TXRF instrumentation used consisted of an x-ray tube in type-D housing, TXRF module, detector and other peripherals which includes x-ray generator, electronic modules for signal processing and a personal computer for spectral data storage and analysis. Figure 3.1 shows a typical block diagram of the TXRF instrumentation setup.

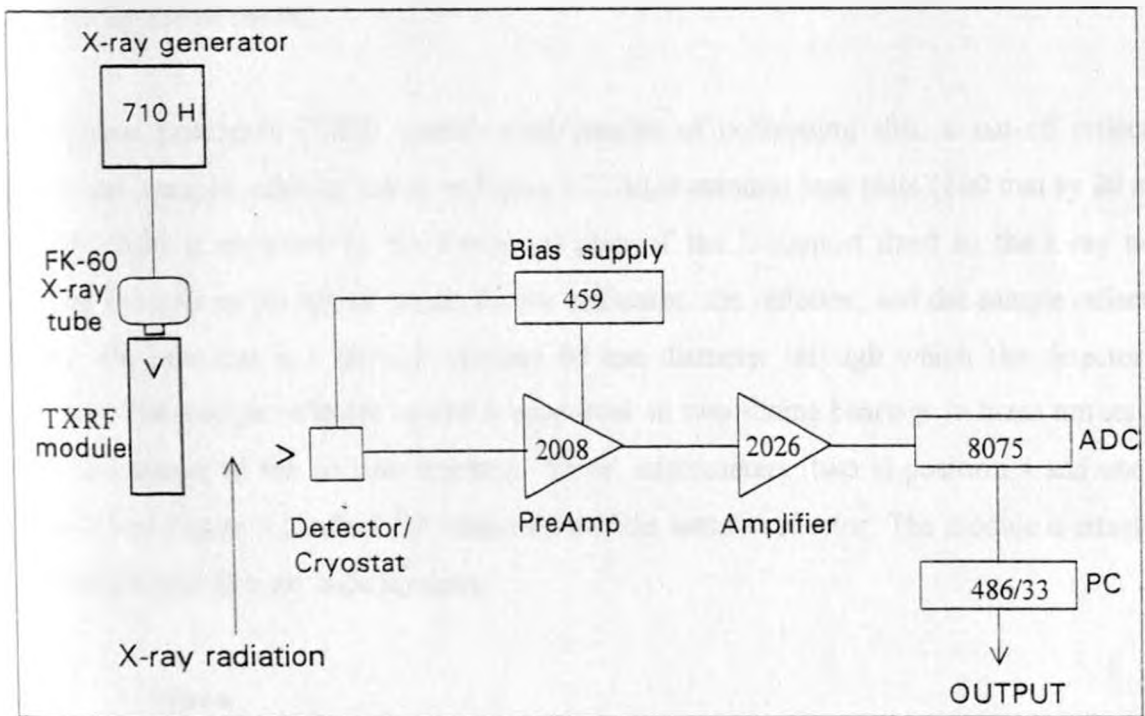
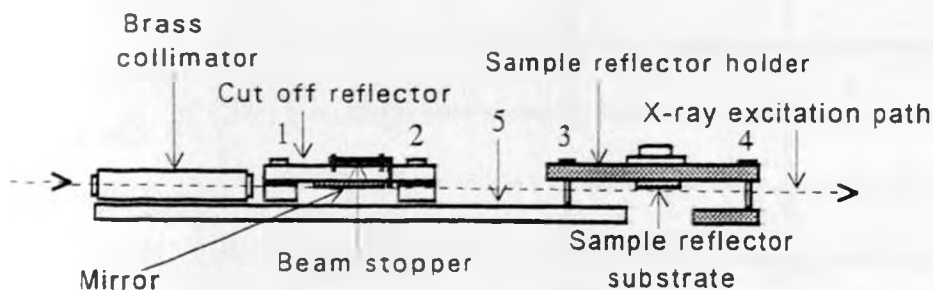


Figure 3.1 Block diagram of a typical TXRF spectrometer

The x-ray generator supplies the high voltage and current required by the x-ray tube for the production of the x-rays. The tube output voltage varies from 20 to 55 kV (internal maximum set to 53.5 kV) and the output current varies from 5 to 40 mA. The Vienna prototype TXRF module (Wobrauschek, 1989) is attached to the x-ray tube house. The x-rays produced are subjected to collimation, reflection and cut-off in the TXRF module before exciting the thin film sample on the reflector. A Canberra Si(Li) detector with an area 30 mm^2 and thickness 5 mm was used for x-ray radiation detection. The detector crystal is located at a distance of 5

mm from the beryllium window of thickness 25 μm and is cooled by liquid nitrogen in a cryostat. The detector is biased at -800 V by the ORTEC 456 Power Supply (0-5 kV). The detector resolution was determined to be 170.0 eV for 5.9 keV manganese K_{α} peak at pulse shaping of 12 μs time. The Canberra 2026 Amplifier (gain 0.5-1k) used incorporates the pile-up rejector (PUR) option and pulse shaping. The amplifier has necessary electronics for pulse shaping and linear amplifying to enable precise pulse height analysis (PHA). The amplifier outputs are converted by the Canberra 8075 ADC to digital form and transferred to an IBM compatible 486/33 PC interfaced to multi-channel analyser (Canberra System-100). The multichannel analyzer sorts the different pulses of the ADC according to pulse height and accumulates them in their respective memory channels. The spectral data is stored and analysed by use of the PC.

The Vienna prototype TXRF module used consists of collimating slits, a cut-off reflector mirror and sample reflector holder in Figure 3.2. An aluminium base plate (100 mm by 20 mm and 450 mm) is mounted on the horizontal plate of the L-support fixed to the x-ray tube housing and acts as the optical bench for the collimator, the reflector, and the sample reflector holder. On one end is a circular opening 60 mm diameter through which the detector is inserted. The sample reflector holder is supported on two sliding bearings in brass turrets set along a diameter of the circular opening. Three micrometers (two in position 4 and one in position 3 of Figure 3.2) allow for adjustments of the sample reflector. The module is attached to Siemen's type-D x-ray tube housing.



- 1, 2 - Adjustment screws
- 3, 4 - Micrometer screws
- 5 - Aluminium base plate

Figure 3.2 Various parts of a basic Vienna prototype TXRF module

3.2 Attachment of the Prototype TXRF Module

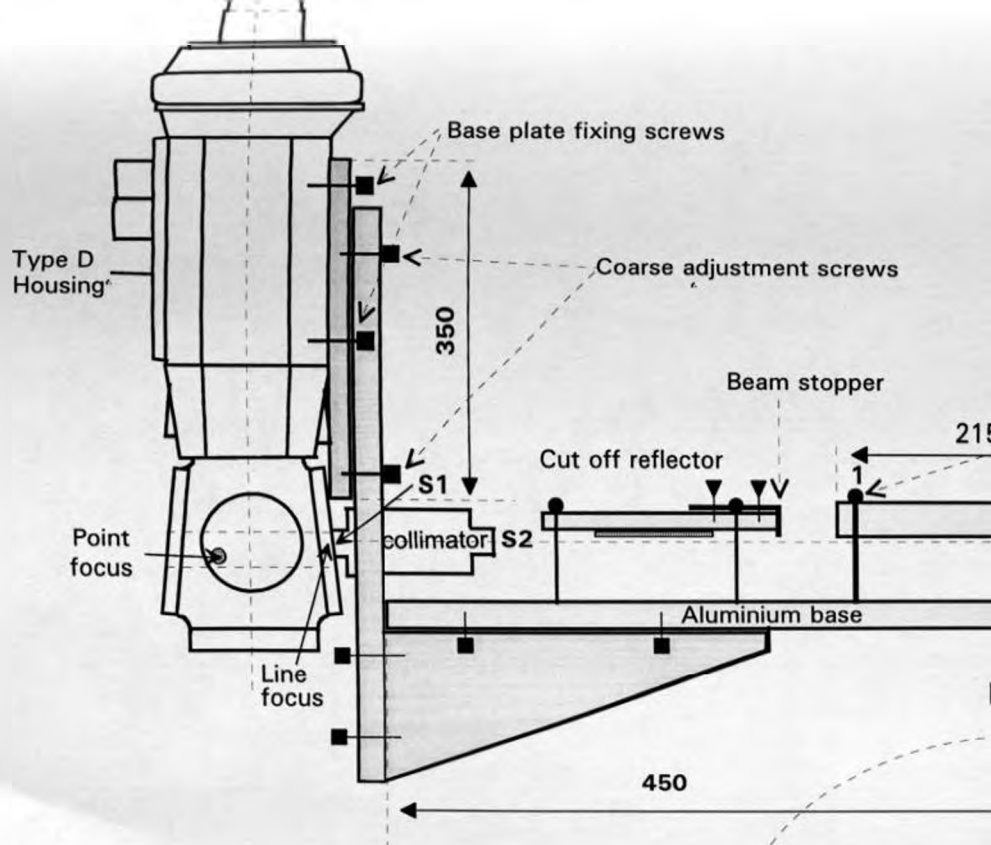
The x-ray tube housing is mounted upright with a 6 degrees deviation from the vertical line. This is due to the emission angle of the tube type, thus the emitted x-ray beam propagates in the horizontal plane. The base plate is fixed with screws to the housing of the tube. The L-shape support is mounted on the base plate and the four coarse adjustment screws used for vertical coarse height adjustment within the alignment groove. The assembly of the TXRF attachment with the Type-D housing is presented in Figure 3.3.

3.2.1 Brass Collimator

The beam collimator is placed close to the tube housing window where the x-rays emerge. It is a brass tube with collimating slits (tantalum) of 1 mm separation located at the ends. The brass collimator is fitted into the tube line focus window of the tube housing. The brass collimator is adjusted by lowering or raising the L-support, while fine adjustment is accomplished by the four screws of the brass plate (Figure 3.3). Rotations of the slit collimator is done to allow parallel adjustment of the emitted beam. For optimum adjustment, an intense rectangular shaped, sharp contrast beam should be observed on the fluorescent zinc sulphide screen located ~50 cm away.

3.2.2 Cut-Off Reflector

The cut-off reflector (50 x 20 x 5 mm) consists of a flat brass piece with the reflector at its centre. The reflector is of Duran-type quartz with a surface quality of $\lambda/20$ and a mean roughness of a few nanometers. Three screws with steel springs allow for adjustment to the desired angle of reflection. The brass piece is pressed with the steel springs against the screw heads and once the reflector is in the correct position, stability is easily maintained. With the zinc sulphide screen positioned at a distance of ~0.5 m away, precise position setting of the reflector is determined. When the reflector is above the beam only a single beam is visible on the screen but on adjusting the reflector first parallel to the beam, then lowering it carefully using the front screws, a reflected beam is observed slightly below the direct beam.



(Dimension in mm)

Figure 3.3 Assembly of TXRF attachment with the

3.2.3 Beam Stopper

Once the two parallel intense beams are distinctly well separated on the screen, the direct beam which contains the high energy photons is 'stopped' by a tantalum absorber such that the reflected beam is propagated alone as shown in Figure 3.4.

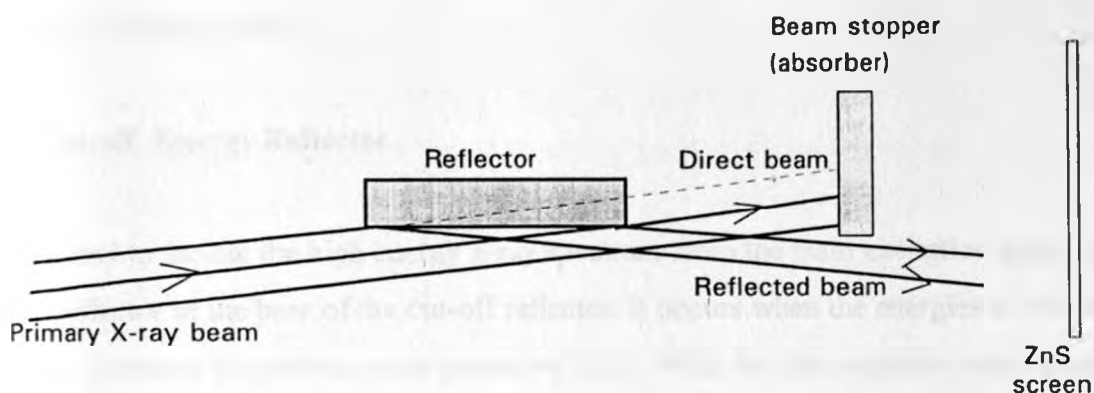


Figure 3.4 Total reflection of low energy x-ray photons and absorption of the high energy non-reflected radiation.

3.2.4 Sample Reflector Holder

The sample reflector holder consists of an aluminium plate with three micrometer screws, the spring load fixing mechanism for the sample carrier, the glides and rotation pieces. The glides fit into the vertical channel of the turrets mounted on the aluminium base plate. This allows vertical and rotational movements for angular adjustment for optimum performance. Once set, further disturbance can be avoided by locking the glides with the over head screws. Sample reflector holder is adjusted to move downwards by turning the micrometer screws counter clockwise. Angular adjustment is accomplished starting from a parallel position of the sample reflector holder where the beam just impinges on the reflector. The adjustment of the sample holder is similar to the cut-off reflector, but the beams having been reflected is going in the opposite direction. To minimize on the scattered radiation from the edges of the sample carrier, the detector is shielded with a lead cap with a narrow opening and the edges coated with indium to absorb the lead (Pb) lines from reaching the detector. This cap restricted the minimum sample carrier-detector distance that could be achieved to ~5.0 mm distance.

3.3 TXRF Module Optimization

3.3.1 Setting of the Tube Current and Voltage

A control sample consisting of titanium, cobalt and strontium was irradiated at different voltage settings at a fixed current of 20 mA. The x-ray tube current value was carefully selected after it was realised that the system overheats at high current values because of inefficient cooling system.

3.3.2 Cut-off Energy Reflector

This is used to isolate the high energy x-ray spectrum from the main excitation beam, using a quartz reflector at the base of the cut-off reflector. It occurs when the energies of the incident photons are above the critical angle (equation 2.21). With the zinc sulphide screen positioned at a distance of ~0.5 m away, precise position and settings of the reflector is determined using the adjustment screws. When the reflector is above the beam only a single beam is visible on the screen. By first adjusting the reflector parallel to the beam, then rotating it carefully using the front screws ('2' in Figure 3.2), a reflected beam is observed slightly below the direct beam.

3.3.3 Sample Reflector Holder

The same principle described in 3.3.1 is applied to adjust the sample carrier bearing in mind that the main purpose of radiation beam at these stage is to excite the sample film deposited on the reflector surface. The highest signal to background ratio is expected when total reflection of the incident beam occur, resulting in the dual excitation of the sample by the incident and the reflected beams (Equation 2.30). Experimentally, this was observed when the two beams on screen were just about to overlap.

3.3.4 Stability of the X-ray Generator during Sample Irradiation.

The stability of the generator is vital in TXRF analysis for reproducibility of the results. Practically, the sensitivity is function of tube high voltage. It is for this reason that different

tube voltages result in different values of sensitivities for the control sample. Normally, it is recommended that the x-ray generator is powered on for several minutes before any measurements are done. This is to allow the system to come to its acquiescent state.

3.3.5 Reduction of Background Radiation through Modification of Excitation Beam using Zirconium Filter.

The primary excitation beam may be modified by filtering it using the housing filters of the tube. This has sometimes been used to improve the detection limits of certain elements due to its lower background of the scattered excitation beam. The resultant excitation beam is more monoenergetic.

3.4 Sample Preparation for TXRF Analysis

Before any sample is subjected for TXRF analysis, appropriate preparation procedures are required depending on the nature and matrix of the sample. Recent application areas are summarised in Table 3.1.

Table 3.1 Recent fields of TXRF application (Stobel and Prange, 1985)

| | | |
|------------------------------|----------|-------------|
| Rain water | Air dust | Lung Tissue |
| River water | Fly ash | Blood serum |
| Sea water | | Hair |
| Suspended particulate matter | Minerals | |
| Sediment | Nodules | Fine roots |
| Algae | | Needles |
| Mussel | Food | Wood |

One of the major advantages of using TXRF as mentioned earlier is that it requires minute quantities of a sample. Samples for TXRF analysis, are normally of two types; aqueous and solid materials, each of which is prepared accordingly as summarised in the following sample preparation flow charts of figure 3.5 and 3.6.

Aqueous samples

(Aliquotation of the sample and internal Co- standardization)

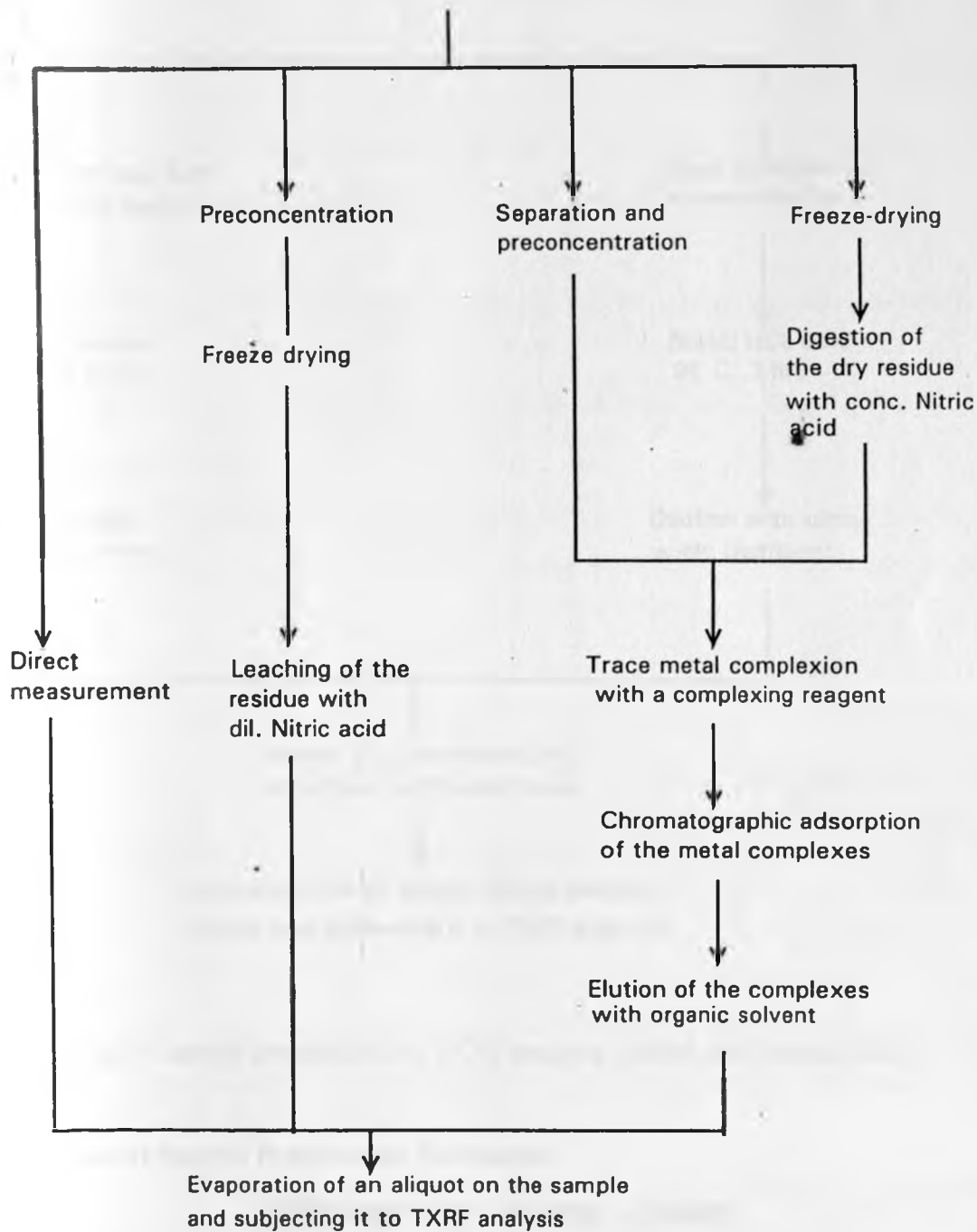


Figure 3.5 Aqueous sample preparation for TXRF analysis (Stobel and Prange, 1985)

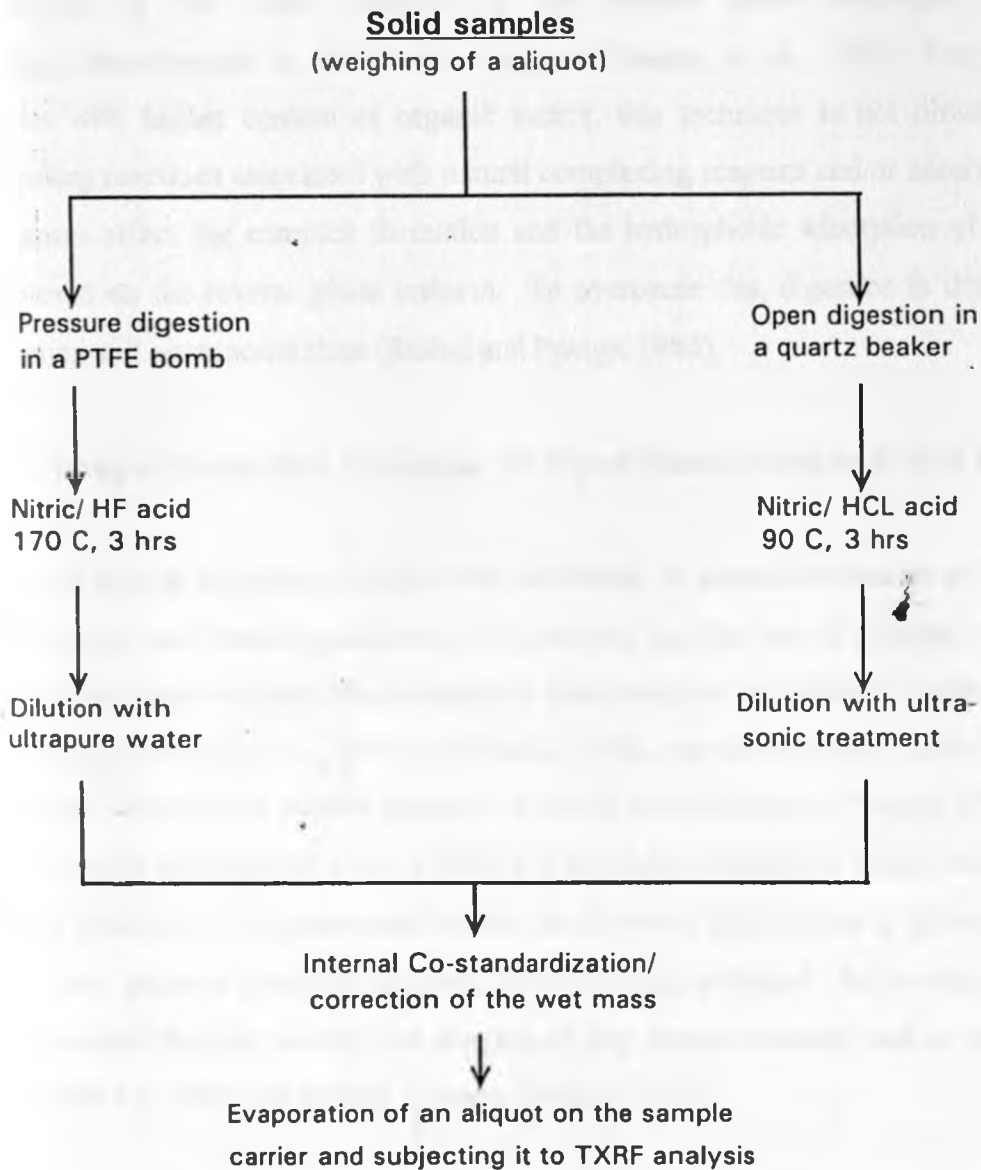


Figure 3.6 Solid sample preparation for TXRF analysis (Stobel and Prange, 1985)

3.4.1 Aqueous Sample Preparation Techniques

UNIVERSITY OF NAIROBI LIBRARY

In most cases, these types of samples require simple preparation techniques such as direct measurement or a physical concentration like freeze drying. This is applicable for samples with no or only small amounts of matrix elements present as in the case for rain water or river water with no organic matter. In cases of high concentrations of low atomic number elements in the matrix, preconcentration procedures are recommended for trace element analysis. A reliable technique for separation of alkalis and alkaline earth elements and the

enrichment of the trace elements is the reverse phase technique with sodium dibenzylidithiocarbamate as complexing reagent (Prange, *et al.*, 1985). For natural water samples with higher content of organic matrix, this technique is not directly applicable. Competing reactions associated with natural complexing reagents and/or natural hydrophobic substances affect the complex formation and the hydrophobic adsorption of the carbonate complexed on the reverse phase column. To overcome this, digestion is done prior to the separation and preconcentration (Stobel and Prange, 1985).

3.4.1.1 Sample Preparation Technique for Direct Measurement and After Freeze Drying

There are typical applications which take advantage of particular features of TXRF such as the ability to use minute quantities of the sample and the use of internal standard. These applications include direct measurement of such samples as rainwater (Stobel *et al.*, 1985), river-water (Prange, *et al.*, 1985; Michaelis, 1983), certain ultrapure fluids or radioactive solutions, where no or minute amounts of matrix elements occur (Prange, 1989). For direct measurement, an aliquot of a few millilitre of an aqueous sample is spiked with a few μl of an internal standard. After a thorough mixing, an aliquot of this solution is spiked on the sample carrier and vacuum dried for analysis. Freeze drying technique for sample preparation is recommended for near matrix free samples of low element content such as rain water, ultra pure fluids e.g. acids and organic solvents (Prange, 1989).

In direct measurement, an aliquot of a few millilitre of an aqueous sample with a few microlitre of standard reference solution added, is thoroughly mixed and an aliquot of (10-50 μl) spiked on a siliconized quartz sample carrier and vacuum dried for TXRF analysis.

3.4.1.2 Sample Preparation by Preconcentration with Sodium Diethyldithiocarbamate

This procedure is used to preconcentrate aqueous samples using sodium diethyldithiocarbamate complexing reagent as described by Prange *et al.* (1985). This technique allows only selected trace elements to be preconcentrated and may not be appropriate for elements that cannot be complexed.

3.4.2 Sample Preparation of Solid Samples

For solid samples preparation, digestion procedures are recommended, (Holynska, 1996). Sample digestion procedures are well developed and widely used in such areas as atomic absorption spectrometry (AAS) and inductively coupled plasma atomic emission spectrometry (ICP-AES), (Sansoni and Iyengar, 1980). For TXRF applications the digestion does not have to be complete, but should give at least fine suspension. However, in the case of combination with subsequent separation and preconcentration, complete digestion is necessary. Complete sample digestion is achieved using pressure digestion Teflon bombs.

3.4.2.1 Pressure Digestion using Teflon Bomb

The samples for digestion are pulverized, thoroughly homogenized and dried to constant weight. Aliquot portion of mass 0.1-0.3 g are placed in the Teflon bomb with proportional amount of nitric acid, sealed tightly and kept in the oven for about 3 hours at about 165 °C (Holynska, 1996). After which the sample is removed and cooled, an internal standard is added and an aliquot portions of 5-10 microlitre spiked on the sample carrier for analysis.

3.5 TXRF Energy Spectrum

Apart from the photopeaks of the sample elements observed in a typical TXRF energy spectrum, a number of other peak structures are observed as a result of the artifacts in the detection mechanism. Since these peaks are not caused by interactions of the sample constituents, have no analytical use and tend to obscure the information content of the spectrum. These peaks include silicon peak from the sample carrier, gold peaks as a result of interaction between the incident radiation and the detector gold contacts. Tungsten peaks may be observed if the Vienna type TXRF module is used. Sum peaks and pile-up effects originating from the electronic pulse counting circuitry are also observed. Sometimes though rare, second order effects from the sample may appear as peaks in the energy spectrum; these include Raman scattering and the radiative Auger effect (Van Espen, 1980).

CHAPTER FOUR

EXPERIMENTAL PROCEDURES

4.1 Optimisation of TXRF Instrumentation

4.1.1 Tube High Voltage

In this section, the procedure used to optimise the x-ray tube high voltage using a control sample at tube constant current of 20 Amps is described. The tube voltage was varied between 20 kV to 50 kV in steps of 5. Intensities of the control sample elements (titanium, cobalt, strontium) were evaluated at different voltages. Intensity values were plotted against the tube voltages. The obtained intensity values were normalised such that values corresponding to the highest voltage (50 kV) were assigned a unit value and the intensities of other voltages were normalised with respect to the values obtained at 50 kV.

4.1.2 Cut-off Energy

Good cut off energy was easily achieved with the cut-off reflector at high tube voltage of 50 kV and 10 Amperes. The cut-off reflector screws were adjusted uniformly to lower the quartz reflector until the incident x-ray beam grazed the reflector surface as noted on the ZnS screen by the abrupt loss of beam intensity. At that point, the '2' screws of the cut-off reflector (Figure 3 2) were very carefully adjusted clockwise to rotate the cut-off reflector to obtain maximum separation and maximum intensities for the reflected and direct beams on the ZnS screen

4.1.3 Beam Stopper

Once the two intense beams were well separated (section 4.1.2), it was easy to cut off the upper direct beam. The beam stopper was lowered to cut across the two beams. It was then slowly raised until only the lower reflected beam was transmitted. The beam stopper screws were then adjusted uniformly so that the reflected beam intensity on the ZnS screen was more intense and uniform while ensuring the total absorption of the direct beam.

4.1.4 Adjustment of Sample Reflector Holder

The same principle of adjustment for the cut-off reflector was applied for the sample carrier holder, bearing in mind that the main purpose of the now modified beam at these stage is to excite the thin sample film deposited on the reflector surface. The highest signal to background ratio was achieved when the reflected and direct beams were just about to overlap on the zinc sulphide screen placed about 0.5 metres away. This was when the sample reflector holder was set such that the angle of the excitation beam was at its minimum.

4.1.5 Modification of Excitation Beam for Spectral Background reduction

To achieve modification of the primary beam, the tube housing filters were used. This was achieved by positioning the desired filter material in the beam path. Two positions of zirconium filter and no filter were selected. Zirconium was chosen because its characteristic energy line is close to that of Molybdenum, thus offering a good filter for low energy Bremsstrahlung radiation.

4.1.6 X-ray Generator Stability

A control sample was irradiated for a maximum of 2000 seconds and analysed at 300 seconds interval. No other experimental parameter was changed during the course of sample measurement. The stability of the x-ray generator was evaluated from multivariate statistical considerations for 'noise' or anomaly of obtained spectral data measurements.

4.1.7 Surface Distribution and Sample Homogeneity

An attempt was made to establish the most ideal and suitable way of improving the sample homogeneity and limit the spreading on the sample carriers without introducing a possible contaminant. In siliconization of sample carriers, about 10 μl of silicon solution (*Serva*) was spiked on cleaned sample carrier and left to dry in the oven for 3 hours at about 85 $^{\circ}\text{C}$. In the technique adopted for this research, the sample carriers were oven dried at about 60 $^{\circ}\text{C}$

4.1.8 Long Term Stability of TXRF Measurements

Long term stability of the TXRF system used was determined from measurements of strontium intensity in a control sample at the start and end of daily measurement sessions for 70 days.

4.1.9 Calibration of TXRF Spectrometer for Elemental Sensitivity and Quantitative Analysis

To carry out qualitative and quantitative analysis, the TXRF spectrometer was calibrated for elemental sensitivity and spectral energy. Calibration of the spectrometer for quantitative analysis was performed using multi-elemental standards of which 10 μ l solutions were spiked on 5 different sample carriers and irradiated for a 1000 seconds at tube settings of 40 kV and 20 mA. From spectra data, elemental sensitivity calibration was obtained, using QXAS-Simple Quantitative Analysis (using an internal standard method) program for K and L-lines. Cobalt was used as the internal reference element in all cases for evaluation of analyte concentrations.

4.2 Cleaning Procedures of Sample Containers, Sample Carriers and Teflon Bombs

4.2.1 Sample Containers

Prior to any sample preparation, a clean working environment was ensured. Polyethylene or polypropylene containers used were thoroughly cleaned to reduce the risk of sample contamination (Iyengar and Sansoni, 1980). Each container was rinsed and then filled with double distilled water followed by the addition of ethylenediaminetetraacetic acid (EDTA) to make a 1-3% solution. Five drops of ammonia was added to raise the pH of the solution to about 9. This solution was heated at 80^o C for 1 hour. The solution was then poured out and the container thoroughly rinsed until the pH of the water used in cleaning was 6. The containers were filled with about 6 % ultrapure nitric acid and kept at 80^o for 1-2 hour, and then rinsed thoroughly with the double distilled water, and finally vacuum dried. The containers were closed and kept in a safe dust free environment.

4.2.2 Teflon PTFE Digestion Bomb

The cleaning procedure used to clean the PTFE bomb was the same as for the sampling containers except for a few modifications. The Teflon cup was thoroughly rinsed with double distilled water. It was then filled with hot 1-3 % freshly prepared basic EDTA solution and kept closed for 2-3 hours in the oven at 85 °C. The cup was then rinsed thoroughly until the pH 6 of the double distilled water used was achieved. Better results were obtained when cleaning was done while the cup was still hot. Depending on the holding capacity of the cup, Suprapure nitric acid was added in the ratio 1 ml of the acid to 8 ml of cup volume. Other metallic parts of the bomb were fitted together as described by the supplier and placed in the oven at 170 °C for 3 hours. After which the bombs were removed and allowed to cooled for at least six hours on a metallic surface for faster heat dissipation. After the bomb had cooled, the contents were shaken, opened and 10 µl of the acid spiked on a clean sample carrier. The bomb "blank" sample carrier was dried in an oven at room temperature and pressure lowered drastically to about 500 mbar to accelerate the process. The bomb "blank" sample was then irradiated for 1000s. If the spectrum obtained from the sample carrier showed any traces of contamination, the cleaning procedures were repeated until a 'clean' spectrum of the bomb "blank" sample was obtained after which the acid was poured out and the bomb rinsed thoroughly until it attained pH 6 of the double distilled water. The bomb was kept closed in a safe environment for sample digestion.

4.2.3 Sample Carriers

The method used was more less the same as the one described in 4.2.2 above with slight modifications. The sample carrier was initially thoroughly cleaned with a white soft Kleenex paper tissue and plenty of double distilled water from a wash-bottle until there was no observable visual stain on their surfaces. Both sides of the carriers were cleaned but emphasis was given to the sample side. Holding each of the carriers with clean plastic tweezers, they were rinsed with plenty of double distilled water after which they were arranged in an arrayed stack, without their surfaces being in contact with each other and placed in a clean polyethylene beaker filled with hot basic freshly prepared 1-2 % EDTA solution. All the carriers were immersed fully in the solution and oven dried at 90 °C for two

hours. The carriers were then removed and immediately thoroughly rinsed with plenty of double distilled water while held by clean plastic tweezers until the final pH of the water used remains constant. Again, the sample carriers were arranged in an arrayed stack, with no two surfaces in contact with one another and immersed in a clean polyethylene beaker filled with 5-10% Suprapure nitric acid solution, and oven dried at 85 °C for another hour. On extracting the carriers from the hot solution, they were thoroughly rinsed with plenty of double distilled water while held by clean plastic tweezers. They were then arranged on a clean plate with the sample deposition side facing up, placed in the oven at about 60 °C and pressure lowered to 400 mbar for 10 hours for drying. The carriers were then kept in a clean covered petri- dish, with the sample side still facing up.

All the sample carriers were screened for contamination by irradiating them for 1000s. If any unexpected peaks were observed in the resulting spectrum, cleaning was repeated until no trace of contamination was observed.

4.2.4.1 Reproducibility of TXRF Analytical Results

A multi-element standard solution was prepared from the stocks of the available standard solutions. Ten replicates of 2-10 µl volume of the sample were spiked on the sample carriers and dried in low pressure chamber. They were then analysed using the same experimental conditions described earlier.

4.2.4.2 Sample Contamination

Because of the high sensitivity of TXRF technique, and the small amounts of sample usually required, extra precaution is necessary at all the stages of sample preparation due to external contamination of the sample. In a case study, a prepared sample on a carrier was left exposed for two weeks in the lab after the initial analysis. It was then re-analysed to determine the extent of contamination from dust particles during the course of this time.

4.3 Sampling and Sample Description

4.3.1 Sampling

4.3.1.1 Water Samples

Water samples were bought randomly from various stores within and outside Nairobi. Tap water was also sampled from a running tap for four consecutive days for this study. Mineral samples bought were contained in polyvinylchloride (PVC) bottles with no visible suspended matter. In Table 4.1 the trade name, codes as well as other details are presented.

Table 4.1 Water samples and their Description

| Trade Name | Code | Description given on the label |
|-------------------------|----------|--|
| Local samples | | |
| <i>Safari</i> | A | Deep water well from within Nairobi area |
| <i>Peria</i> | B | Deep water well from the environs of Nairobi |
| <i>Mountken</i> | C | Deep well water from within Nairobi area |
| <i>Wozone</i> | D | Spring water from within Nairobi area |
| <i>GreatRift</i> | E | Natural hot spring water from the Rift Valley |
| <i>Highland</i> | F | Natural spring water from Central Kenya |
| <i>Aquanova</i> | G | Pure mountain spring water from Central Kenya |
| <i>Keringet</i> | H | Natural spring water from high altitude conservation zone in Kenya's Rift Valley |
| <i>Mt Kilimanjaro</i> | I | Natural spring water from the slopes of Mt Kilimanjaro (Mzima) |
| Imported samples | | |
| <i>Mount Frankline</i> | K | Natural spring water from near a mountain in Australia |
| <i>Ice Mountain</i> | L | Fountain spring water from Alton, North America; |
| <i>Evian</i> | M | Natural spring water from the French Alps |
| <i>Vittel</i> | N | Spring water from a conserved site in Vosges region, Eastern France |

4.3.1.2 Maize Samples

Three 2 kg packets of the three major brands of maize flour: *Hostess, Jogoo and Ugali* were bought randomly from various supermarkets. Each packet was homogenized with a clean

constant weight to eliminate the moisture content. A portion of the sample ~1 gram was weighed for digestion. Three different kinds of fresh maize grains were dried to constant weight and later grounded to powder form and digested.

4.3.1.3 Tea Samples

Nine 100 grams packet of Kenya tea leaves (*Ketepa*) were bought randomly from various shops. Each packet was homogenized with a clean plastic spoon before taking an aliquot of 1-3 grams for oven drying at 90 °C to constant weight. The amount needed for digestion was weighed and digested. Three tin containers each 100 grams of instant tea were also purchased, from which 1-3 gram of sample were taken from each tin and dried to constant mass before digesting.

4.3.1.4 Kale Samples

Ten fresh vegetables kale leaf samples were purchased randomly from different vendors in Nairobi. They were rinsed thoroughly with double distilled water before they were dried at oven at 90 °C to constant weight. The samples were later grounded to fine powder with a pestle and a mortar before digestion.

4.3.2 Sample Preparation for Analysis

4.3.2.1 Water Samples

The procedure used for water sample preparation was as follows: One millilitre of the sample was pipetted onto a clean vial. A few mls of the sample were used to rinse the vial into which the sample was to be placed. Also to minimise contamination, the pipette used was rinsed three times with the same sample. 10 µl of prepared (100 µg/g) cobalt internal standard was added i.e. corresponding to internal standard concentration of 1µg/g cobalt to 1 ml of the sample. The content of the vial was mixed thoroughly by shaking and 10 µl was spiked on a clean sample carrier. It was observed that the samples spread to about 6 mm in diameter. This was dried in a low pressure at room temperature (23 °C) before measurement. The samples were prepared in triplicates.

4.3.2.2 Preconcentration with Sodium Diethyldithiocarbamate (NaDDTC)

The following procedure was used for preconcentrating the mineral water samples (Holynska, 1996): A 100 ml sample was taken, an internal standard and a carrier added then the pH adjusted to between 5 and 6, and 10 ml of freshly prepared 2% sodium diethyldithiocarbamate (NaDDTC) solution was added and content the thoroughly mixed. After 15 minutes, the precipitate formed was filtered through Millipore filter of pore size 0.4 μm . The filter with the precipitate was placed in clean beaker and dissolved out in a clean container using 1 ml of Methyl Iso-butyl Ketone (MIBK). After the precipitate had completely dissolved, the filter was removed. A solution of 10 μl from this preconcentrated sample was spiked on a clean sample carrier for analysis.

4.3.2.3 Maize, Tea and Kale Samples

The pulverized and dried samples were thoroughly homogenized using clean non-metallic tools. Between 0.1-0.3 grams (in the ratio of 0.1 grams to 4.0 ml of Suprapure nitric acid of the sample) was put into the Teflon bomb cup, sealed tightly and heated in the oven for about 3 hours at about 170 $^{\circ}\text{C}$. This ensured that there was adequate vapour space when fully charged to enable the digestion to proceed without unusual hazards. After cooling, an aliquot of 10 μl of sample was taken for measurement to check for cobalt. The volume of cobalt internal standard added depended on the initial dry weight of the sample and the expected elemental concentrations of sample. A homogeneous mixture of the sample and the internal standard was ensured by thorough mixing. Three replicates of 10 μl portions of the digested samples were prepared for the analysis.

4.3.2.4 Sample Irradiation

Because of the inefficient cooling system of the x-ray tube encountered at the initial stages of the research when operating at high currents, the following x-ray tube operating conditions were used: 40 kV for high voltage and 20 mA for current. Samples were irradiated for 2000 seconds.

CHAPTER 5 RESULTS AND DISCUSSION

5.1 Optimisation Results

5.1.1 Tube High Voltage

Figure 5.1 shows how the tube high voltage affects the peak to background ratios of the control sample elements.

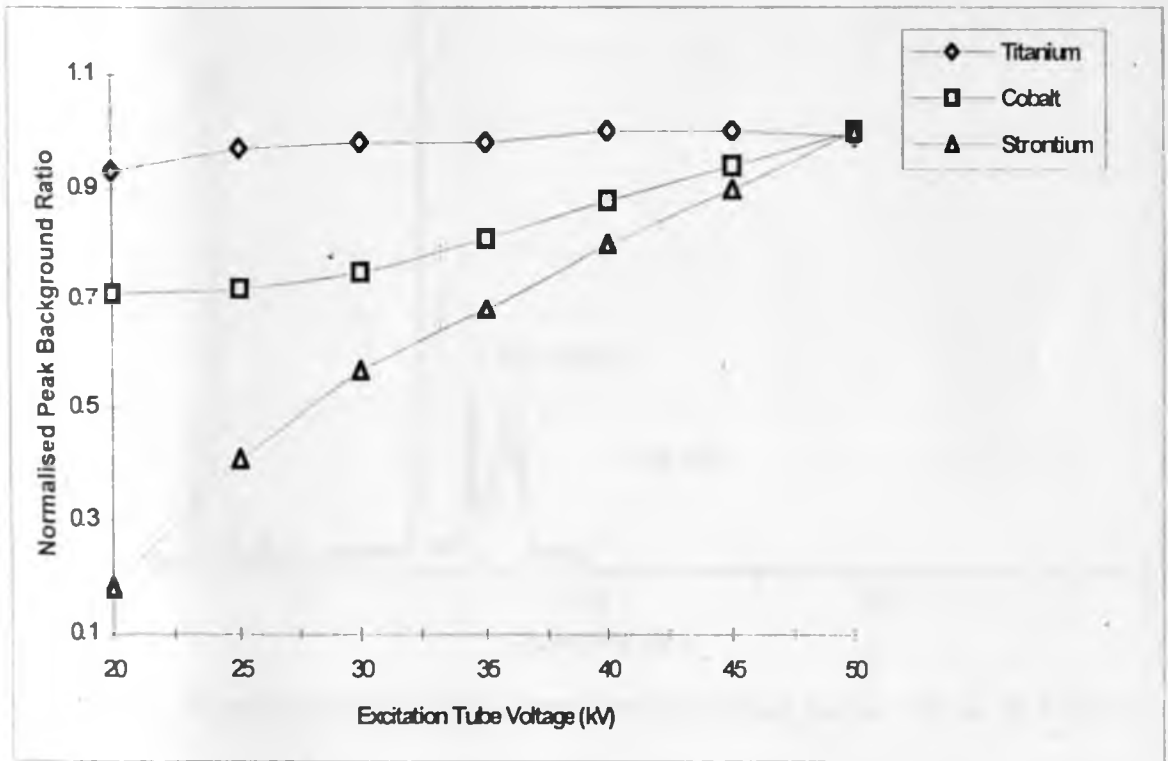


Figure 5.1 Variation of normalised peak to background ratio of titanium, cobalt and strontium at different operating voltages, current set at 20 mA.

From Figure 5.1, high voltage tube settings significantly influence the strontium and cobalt peak intensities in the control sample. Titanium photopeaks located in the lower part of the energy spectrum (~4.5 KeV) is least affected by variation of the tube voltage. The characteristic energies of the elements in the control sample range from low to high in the typical TXRF spectrum energy. Optimum operating conditions for the tube voltage which resulted in high signal to background ratio were observed at over 35 kV.

5.1.2 Cut off Energy for Bremsstrahlung Radiation

The cut off energy achieved was 20.0 KeV with little or no counts on the upper part of energy spectrum after optimisation of the various components of TXRF module. Figure 5.2. show the peaks from the control sample carrier.

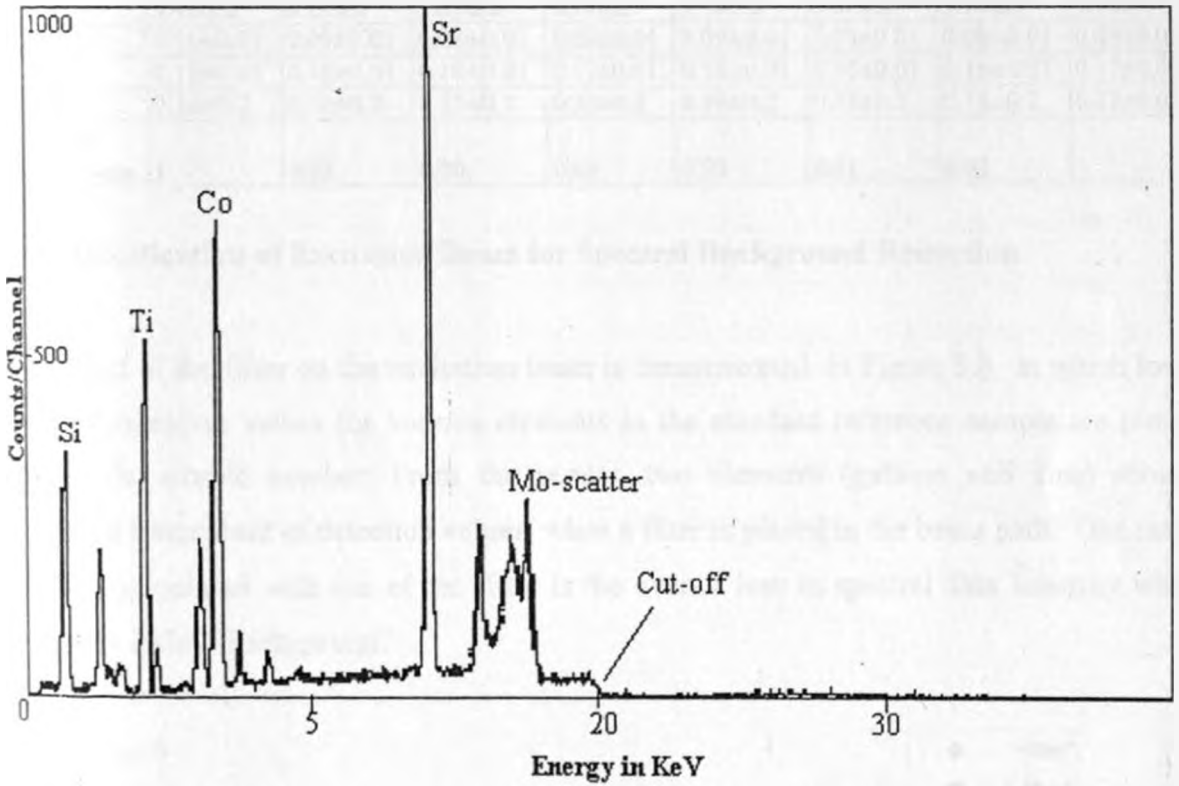


Figure 5.2 Spectrum showing high energy Bremsstrahlung the cut-off at 20.0 KeV.

5.1.3 X-ray Generator Stability

Table 5.1 shows the results of analysis of a sample at various counting times. The results show that a high deviation (8%) in analyte concentration values occurs within the **first** 300 seconds of counting. This may have been due to low peak counts and high statistical errors of the determined concentration or instability of x-ray generation. For high counting times, the deviations in concentration values were within 2% standard deviation.

Table 5.1 Variation of analyte concentration ($\mu\text{g/ml}$) with time in seconds.

| Time Element | 300 | 600 | 900 | 1,200 | 1,500 | 1,800 | 2,000 | Mean \pm 1sd |
|------------------------------|-----------------|-----------------|-----------------|-----------------|-----------------|-----------------|-----------------|-----------------|
| K | 20.7 \pm 1 | 18.8 \pm 1 | 18.8 \pm 1 | 19.1 \pm 1 | 19.3 \pm 1 | 18.9 \pm 1 | 19.0 \pm 1 | 19.2 \pm 0.7 |
| Ca | 46.2 \pm 2 | 42.2 \pm 2 | 41.8 \pm 2 | 43.3 \pm 2 | 43.6 \pm 2 | 43.3 \pm 2 | 43.5 \pm 2 | 43.4 \pm 1.4 |
| Ti | 3.3 \pm 0.2 | 3.1 \pm 0.2 | 3.0 \pm 0.2 | 3.1 \pm 0.2 | 3.1 \pm 0.2 | 3.1 \pm 0.2 | 3.1 \pm 0.2 | 3.1 \pm 0.1 |
| Mn | 3.3 \pm 0.2 | 3.0 \pm 0.2 | 2.9 \pm 0.2 | 3.0 \pm 0.2 | 3.0 \pm 0.2 | 3.0 \pm 0.2 | 3.0 \pm 0.2 | 3.1 \pm 0.1 |
| Fe | 37.4 \pm 2 | 33.9 \pm 2 | 33.5 \pm 2 | 34.7 \pm 2 | 34.9 \pm 2 | 34.6 \pm 2 | 34.9 \pm 2 | 34.8 \pm 3.6 |
| Cu | 1.5 \pm 0.1 | 1.4 \pm 0.1 | 1.4 \pm 0.1 | 1.5 \pm 0.1 | 1.4 \pm 0.1 | 1.4 \pm 0.1 | 1.4 \pm 0.1 | 1.4 \pm 1.3 |
| Zn | 3.4 \pm 0.2 | 3.0 \pm 0.2 | 3.0 \pm 0.2 | 3.1 \pm 0.2 | 3.1 \pm 0.2 | 3.0 \pm 0.2 | 3.1 \pm 0.2 | 3.1 \pm 0.1 |
| Br | 0.11 \pm 0.01 | 0.09 \pm 0.01 | 0.08 \pm 0.01 | 0.09 \pm 0.01 | 0.09 \pm 0.01 | 0.08 \pm 0.01 | 0.08 \pm 0.01 | 0.09 \pm 0.01 |
| Sr | 0.19 \pm 0.01 | 0.18 \pm 0.01 | 0.18 \pm 0.01 | 0.17 \pm 0.01 | 0.16 \pm 0.01 | 0.16 \pm 0.01 | 0.16 \pm 0.01 | 0.17 \pm 0.01 |
| Pb | 0.36 \pm 0.2 | 0.36 \pm 0.2 | 0.35 \pm 0.2 | 0.38 \pm 0.2 | 0.39 \pm 0.2 | 0.38 \pm 0.2 | 0.39 \pm 0.2 | 0.37 \pm 0.02 |
| Normalised/ weighted mean | 1 | 0.92 | 0.90 | 0.93 | 0.93 | 0.91 | 0.92 | |

5.1.4 Modification of Excitation Beam for Spectral Background Reduction

The effect of the filter on the excitation beam is demonstrated in Figure 5.3 in which lower limit of detection values for various elements in the standard reference sample are plotted against the atomic number. From the results, two elements (gallium and zinc) showed improved lower limit of detection values, when a filter is placed in the beam path. One major problem associated with use of the filter is the overall loss in spectral data intensity which inundates its low background.

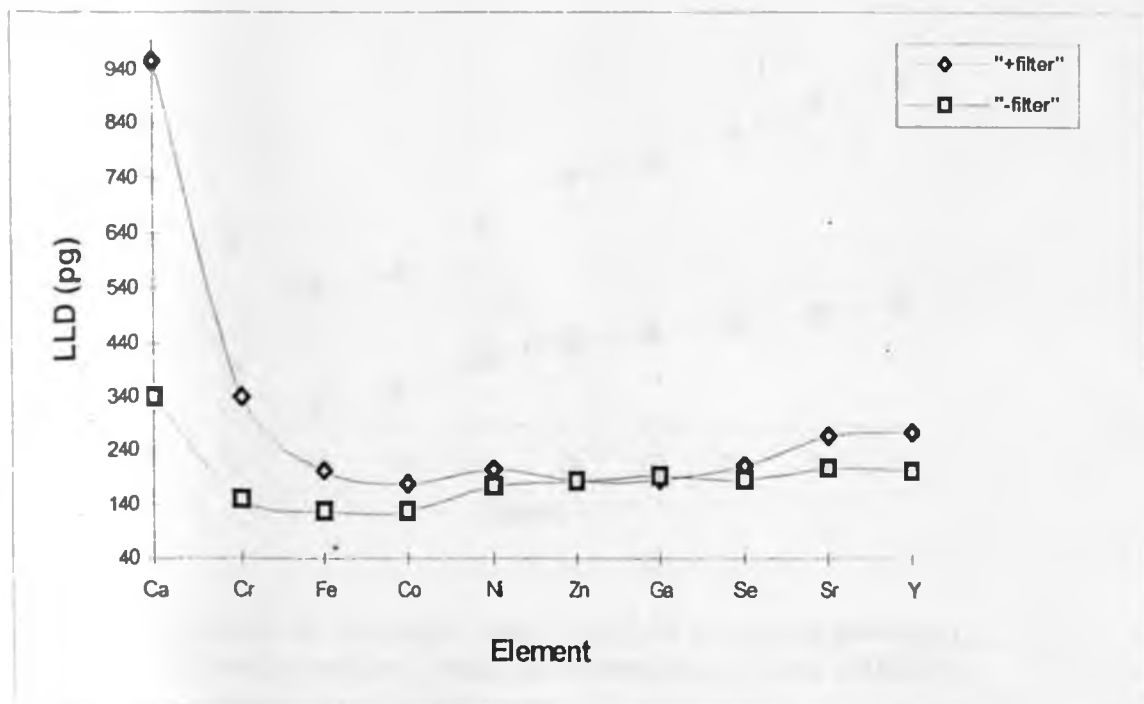


Figure 5.3 Variation of detection limits in pg with (+) and without (-) zirconium filter for molybdenum tube excitation source in TXRF

For low atomic number elements (Z), excitation is mainly due to the low energy photons of the excitation beam consequently the filtering effects of the zirconium filter attenuates the radiation resulting in the increases of the lower limits of detection values.

5.1.5 Surface Distribution and Sample Homogeneity

The major problem with sample carrier siliconization is inherent sample conglomeration which results in high spectral background. The spreading was limited to less than a millimeter radius yet this is a critical factor for effective sample excitation. For efficient sample excitation, the sample needs to spread to less than 7 mm in diameter on the sample carrier. The consequence of the sample conglomeration results in low intensities of the analytes and enhanced scattering by the sample which increases the detection limits (Figure 5.4).

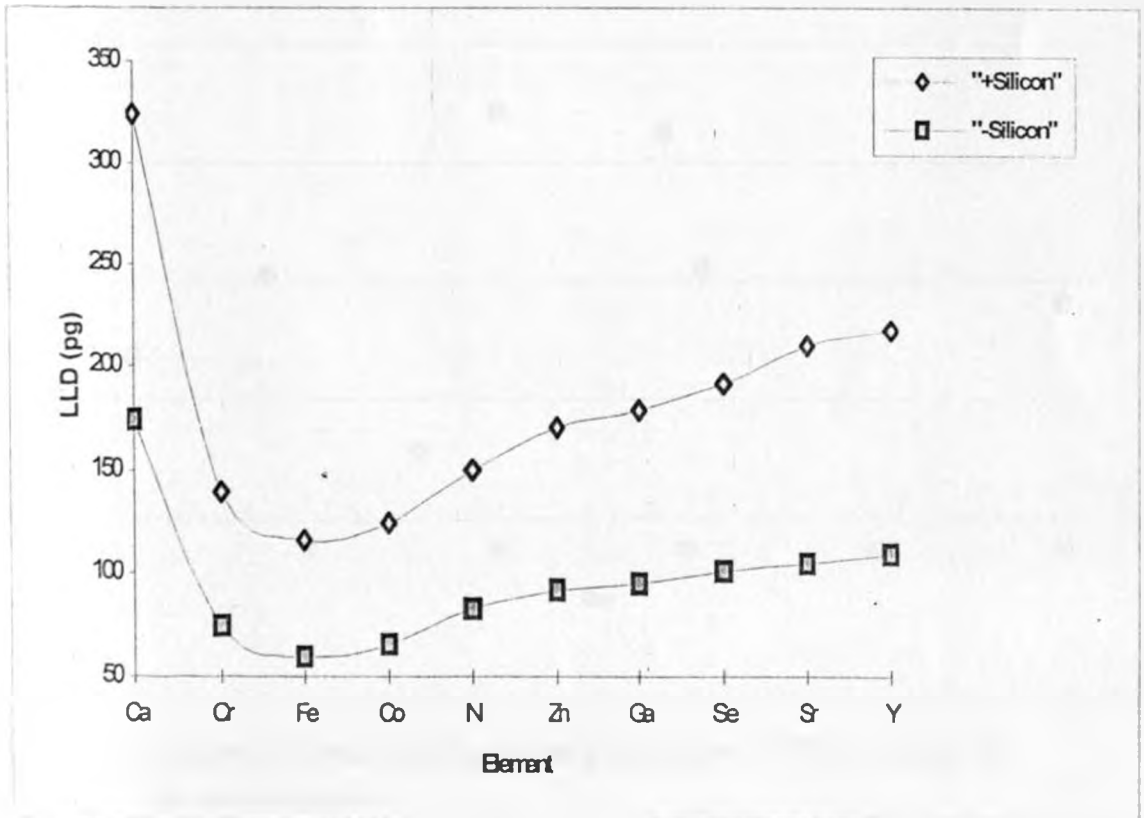


Figure 5.4 Variation of detection limit (in pg) for a standard solution, on siliconized carrier (+) and non siliconized (-) (Time 1000s).

The sample preparation method used throughout this work (drying the sample carriers at 60 °C overnight at low pressures of ~400 mbars) resulted in a natural siliconization of the

carriers, such that samples spiked were homogeneously spread in thin film to 5-6 mm.. Comparison of the lower limit of detection values obtained from sample carriers dried under these conditions and those subjected to siliconization indicates improved values for most elements by a factor of 2-3.

5.1.6 Long Term Stability of TXRF Measurements

Figure 5.5 shows the variation of intensities of the strontium-K α counts during two busy months. The variation from the mean value (3730) within the period does not exceed two standard deviations (2%). Changes to the sample carrier settings normally adversely affect photopeaks located close to the scatter peaks. Strontium K-lines are strategically located near the molybdenum peaks and are good indicators of possible disturbance in the measuring system.

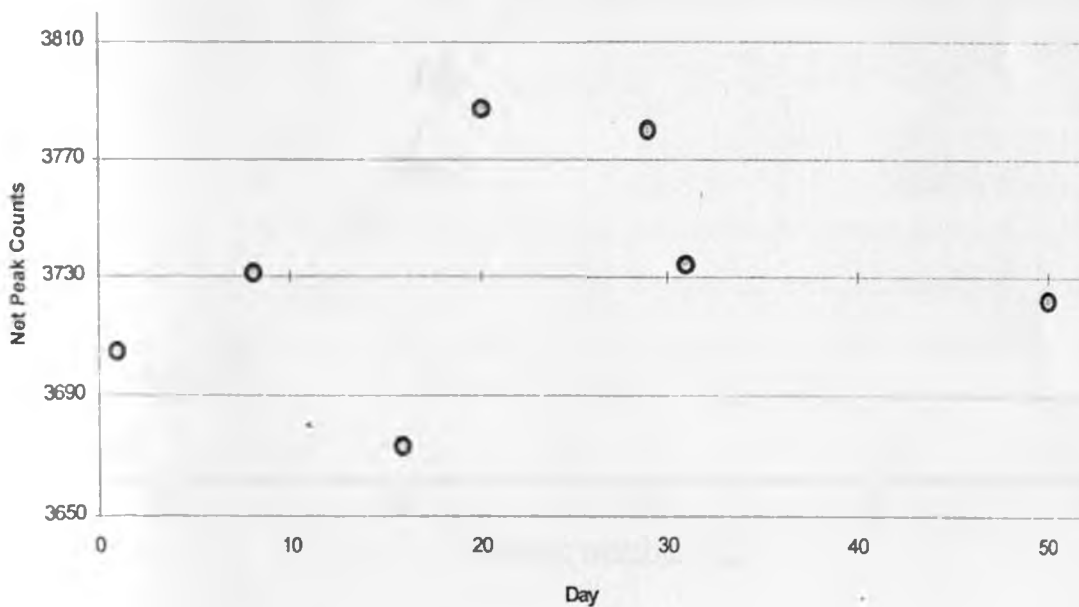


Figure 5.5 Variation of strontium-K α net peak counts over a 70 day period for the control sample.

Further investigation carried out established that the observed instability was probably caused by the orientation of the sample carrier to within two standard deviations. Similar trends were observed when the sample carrier with the control sample, was rotated through small angles up to 360 degrees.

5.1.7 Sensitivity Calibration for the TXRF Measurements

Figure 5.6 shows variation of the relative elemental sensitivities (K-lines) against their atomic numbers. Elemental sensitivity is observed to increase with atomic number up to zinc thereafter tending to a constant value. Concentrations of unknown analytes in the sample are evaluated according to equation 2.31 presented earlier.

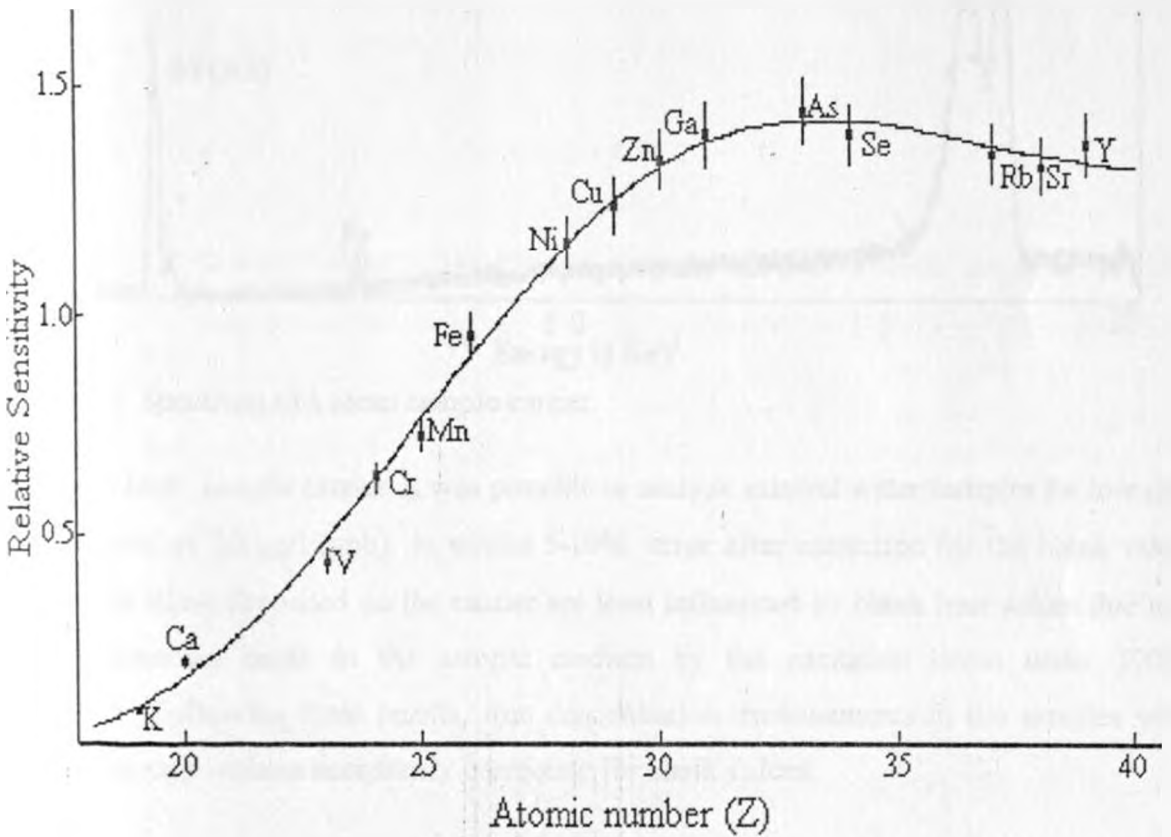


Figure 5.6 Variation of relative elemental sensitivities with the corresponding atomic number for K-lines.

5.1.8 Cleaning of the Sample Carriers

Figure 5.7 shows a spectrum of a blank (cleaned sample carrier)

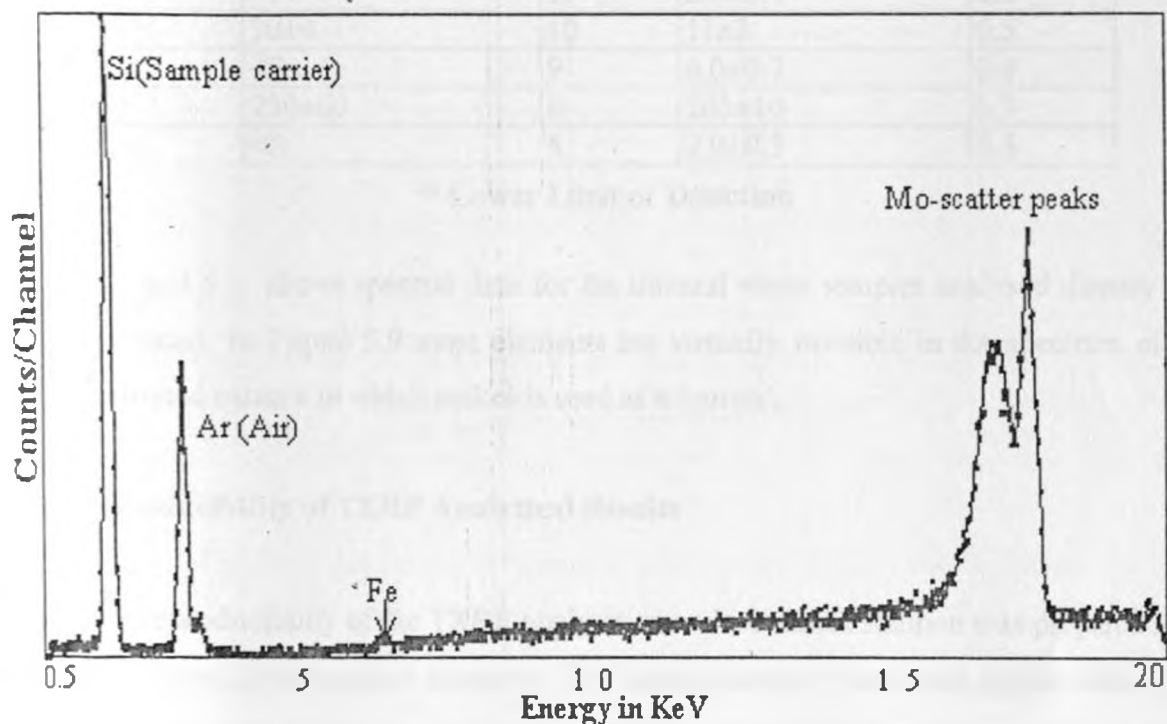


Figure 5.7 Spectrum of a clean sample carrier.

With the 'clean' sample carrier, it was possible to analyze mineral water samples for low iron concentration as 20 $\mu\text{g/l}$ (ppb) to within 5-10% error after correction for the blank value. The sample films deposited on the carrier are least influenced by blank iron values due to a small penetration depth in the sample medium by the excitation beam under TXRF conditions. Following these results, iron concentration measurements in the samples were accurate enough without necessarily correcting for blank values.

5.2 Results of TXRF Analysis of Samples Prepared by Preconcentration Technique with NaDDTC

This technique is selective of a few trace metals and is therefore inappropriate to the study where the interest is wide. In the determination of trace metals of samples prepared by preconcentration technique, the limits of detection were greatly improved as compared to direct analysis method for a sample of mineral water (Table 5.2). Though recovery corrections were not applied to the elemental concentrations obtained from preconcentration technique, iron concentration values were above detection limits in both cases:

Table 5.2 Comparison of results for direct and preconcentrated sample preparation techniques in $\mu\text{g/g}$ for sample J.

| Element | Direct measurement | LLD* | Preconcentrated | LLD* |
|---------|--------------------|------|-----------------|------|
| Cr | <17 | 17 | 2.0±0.4 | 0.8 |
| Ti | 30±4 | 10 | 11±2 | 0.5 |
| Mn | <9 | 9 | 6.0±0.7 | 0.4 |
| Fe | 230±60 | 8 | 205±10 | 0.3 |
| Cu | <8 | 8 | 2.0±0.3 | 0.3 |

* Lower Limit of Detection

Figure 5.8 and 5.9 shows spectral data for the mineral water samples analysed directly and preconcentrated. In Figure 5.9 most elements are virtually invisible in the spectrum of the preconcentrated sample in which nickel is used as a 'carrier'.

5.2.2 Reproducibility of TXRF Analytical Results

To test for reproducibility of the TXRF analysis, a multi-element solution was prepared from the stocks of available standard solutions. Ten sample carriers were each spiked with 10 μl of the multi-element solution and analysed. The results obtained are summarized in Table 5.3

Table 5.3 Comparison of experimental and expected values of multi-elemental standards solutions (n=10).

| Element | Experimental value ($\mu\text{g/ml}$) | Theoretical value ($\mu\text{g/ml}$) | % Error |
|---------|---|--|---------|
| Fe | 9.6±1.5%* | 10.0 | -4.4 |
| Ni | 4.02±0.7% | 4.0 | +0.5 |
| Cu | 1.95±2.0% | 2.0 | -2.5 |
| Zn | 3.00±1.3% | 3.0 | 0.0 |
| Sr | 1.09±2.8% | 1.0 | +9 |
| Ag | 25.0±8.0% | 20.0 | +25 |
| Sn | 9.4±3% | 10.0 | -6 |
| Ba | 6.0±5.0% | 6.0 | 0.0 |
| Pb | 3.10±1.6% | 3.0 | +3.3 |

* standard deviation determined from 10 replicates (%).

The results show good precision, reproducibility and accuracy for most of the analytes to within 6% error margin except for strontium and silver whose values were relatively poor, 9% and 25% respectively.

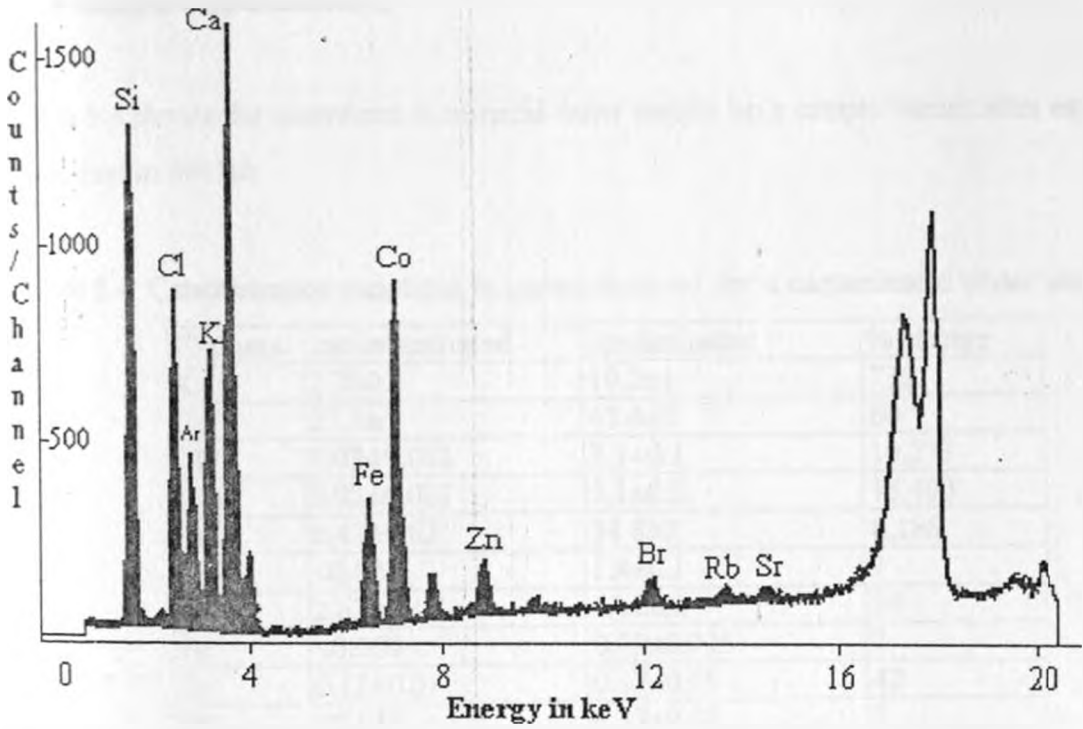


Figure 5.8 A spectrum of mineral water collected for 1000s using direct method of measurement.

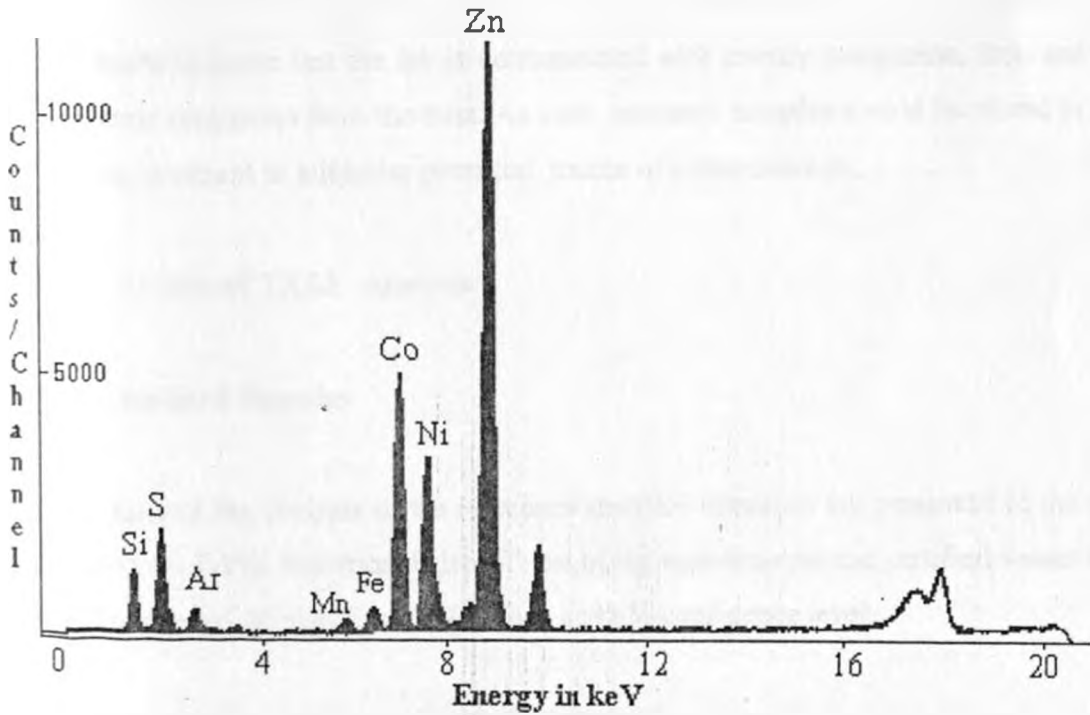


Figure 5.9 Spectrum of the same sample under similar conditions but preconcentrated.

The characteristic x-ray energy line for silver overlaps with that of argon and the error observed could be a result of poor energy peak deconvolution.

5.2.3 Sample Contamination

Table 5.4 shows the alterations in mineral water sample on a sample carrier after exposure to floor dust in the lab.

Table 5.4 Concentration variations in $\mu\text{g/ml}$ observed for a contaminated water sample.

| Element | uncontaminated | contaminated | % change |
|---------|------------------|------------------|----------|
| K | 2.3 ± 0.1 | 19.2 ± 1 | 735 |
| Ca | 27.3 ± 1 | 43.4 ± 2 | 60 |
| Ti | 0.03 ± 0.002 | 3.1 ± 0.2 | 10,233 |
| Mn | 0.02 ± 0.001 | 3.1 ± 0.2 | 15,400 |
| Fe | 0.42 ± 0.02 | 34.8 ± 2 | 8,186 |
| Cu | <0.008 | 1.4 ± 0.1 | ? |
| Zn | 2.63 ± 0.1 | 3.1 ± 0.2 | 18 |
| Br | <0.009 | 0.09 ± 0.005 | ? |
| Sr | 0.12 ± 0.01 | 0.17 ± 0.01 | 42 |
| Pb | <0.015 | 0.37 ± 0.02 | ? |

(? - undeterminable)

This results indicate that the lab is contaminated with mostly manganese, iron and titanium that mainly originates from the dust. As such, prepared samples should be stored in a closed, clean environment to minimise potential source of contamination.

5.3 Results of TXRF Analysis

5.3.1 Standard Samples

The results of the analysis of the reference standard materials are presented in the following Tables (5.5 - 5.10). Statistical Paired T-test of the experimental and certified values for all the samples showed no significant difference at 95 % confidence level.

Table 5.5 Comparison of experimental and certified values in $\mu\text{g/g}$ for Lyophilised Pig Kidney (BCR No. 186). (n=3)

| Element | Experimental value | Certified value | LLD* |
|---------|--------------------|-----------------|------|
| Mn | 7.4±0.4 | 8.5±0.3 | 0.7 |
| Fe | 275±11 | 299±10 | 0.8 |
| Cu | 31.6±0.5 | 31.9±0.4 | 1.4 |
| Zn | 134±6 | 128±3 | 1.4 |
| Se | 9.7±0.5 | 10.3±0.5 | 1.4 |

(* Limits of Detection)

Table 5.6 Comparison of experimental and certified values of concentration in $\mu\text{g/g}$ for Chinese Human Hair (GBW 09101). (n=3)

| Element | Experimental value | Certified value | LLD* |
|---------|--------------------|-----------------|------|
| Ca | 1022±69 | 1090±721 | 2.7 |
| Cr | 3.2±0.3 | 4.8±0.4 | 0.9 |
| Mn | 3.6±1.0 | 2.9±0.2 | 0.7 |
| Fe | 71.0±5 | 71.2±6.6 | 0.8 |
| Ni | 3.4±0.2 | 3.2±0.4 | 1.3 |
| Cu | 23.0±0.8 | 23.0±1.4 | 1.4 |
| Zn | 194±5 | 189±8 | 1.5 |
| Sr | 5.7±0.5 | 4.2±0.1 | 2.4 |
| Pb | 11±1 | 7.2±0.7 | 5.2 |

(* Limits of Detection)

Table 5.7 Comparison of experimental and certified concentration values in $\mu\text{g/g}$ of concentration for Rye Flour (IAEA/ V-8). (n=3)

| Element | Experimental value | Certified value | LLD* |
|---------|--------------------|-----------------|------|
| K | 2320±191 | 1925±135 | 1.3 |
| Ca | 142±4 | 149±10 | 0.5 |
| Mn | 2.1±0.1 | 2.06±0.12 | 0.1 |
| Fe | 5.3±0.5 | 4.1±0.7 | 0.1 |
| Cu | 0.75±0.03 | 0.95±0.19 | 0.3 |
| Zn | 2.65±0.2 | 2.53±0.33 | 0.2 |
| Br | 0.31±0.1 | 0.38±0.07 | 0.2 |
| Rb | 0.55±0.04 | 0.48±0.07 | 0.2 |

(* Limits of Detection)

Table 5.8 Comparison of experimental and certified values in $\mu\text{g/g}$ for 'Rice-unpolished' (NIES No. 10 (a)). (n=3)

| Element | Experimental value | Certified value | LLD* |
|---------|--------------------|-----------------|------|
| K | 1875 \pm 73 | 2800 \pm 80 | 5 |
| Ca | 100 \pm 4 | 93 \pm 3 | 3 |
| Mn | 31.3 \pm 0.7 | 34.7 \pm 2 | 0.5 |
| Cu | 7.9 \pm 0.2 (?) | 3.5 \pm 0.3 | 0.6 |
| Zn | 24.8 \pm 0.5 | 25.2 \pm 0.8 | 0.6 |
| Rb | 4.4 \pm 0.4 | 4.5 \pm 0.3 | 0.6 |

(* Limits of Detection)

Table 5.9 Comparison of experimental and certified values of concentration in $\mu\text{g/g}$ for Japanese Tea (NIES No. 7). (n=3)

| Element | Experimental value | Certified Value | LLD* |
|---------|--------------------|-----------------|------|
| K | 18850 \pm 784 | 18600 \pm 700 | 10 |
| Ca | 3131 \pm 22 | 3200 \pm 120 | 7 |
| Mn | 627 \pm 10 | 700 \pm 25 | 1.4 |
| Ni | 4.6 \pm 0.3 | 6.5 \pm 0.3 | 1.4 |
| Cu | 6.3 \pm 0.3 | 7.0 \pm 0.3 | 1.4 |
| Zn | 35.8 \pm 1 | 33.0 \pm 3 | 1.4 |

(* Limits of Detection)

Table 5.10 Comparison of experimental and certified concentration values in $\mu\text{g/g}$ for Kale reference standard (IAEA/ S636F). (n=3)

| Element | Experimental value | Certified value | LLD* |
|---------|--------------------|------------------|------|
| K | 25909 \pm 2922 | 24370 \pm 1452 | 15 |
| Ca | 38914 \pm 4383 | 41060 \pm 2220 | 9 |
| Mn | 15.4 \pm 0.8 | 14.8 \pm 1.68 | 2 |
| Fe | 81.5 \pm 8 | 119.3 \pm 14.8 | 2 |
| Cu | 3.4 \pm 0.9 | 4.9 \pm 0.63 | 2 |
| Zn | 32.0 \pm 2 | 32.3 \pm 2.8 | 2 |
| Br | 15.0 \pm 2 | 24.9 \pm 2.5 | 2 |
| Rb | 57.3 \pm 5 | 53.4 \pm 5.5 | 2 |
| Sr | 76.4 \pm 6 | 75.7 \pm 29.3 | 1 |

(* Limits of Detection)

The results of analysis of certified reference standards indicated that the analytical technique used is suitable for elemental analysis of digested samples of biological origin with no significant differences at 95% confidence level. For most of the samples analysed, the elemental concentration determined lie within the range of the certified values (>90%) except for a few cases. Notable ones are, copper in the 'Rice-unpolished' and bromine in the Kale standard. The discrepancies in concentration levels in these of the samples may be attributed

to the following reasons:

- (i) Sample preparation method used; for example digestion procedure is known to lower the concentration levels of bromine in most samples;
- (ii) Sample homogeneity;
- (iii) Assumption of a thin sample; in cases of high concentration of sulphur, calcium, potassium or similar atomic number elements modify the calibration curve.
- (iv) Assumption of homogenous internal standard, this can result in a systematic error, easily detected in cases where all the experimental values shift higher or lower than the certified values with equal magnitude.
- (v) sample contamination, most likely to occur on the sample carrier due to dust or other chemicals in the laboratory.

5.3.2 Food Samples

(a) Maize Flour

The elemental concentrations levels in raw Maize were in most cases higher when compared to the processed Maize flour, especially for potassium, zinc and rubidium. In the analysis of the three brands of processed Maize flour and raw Maize, it was observed that the levels for most of the elements seemed to follow the quality of processing. *Hostess*, the highest quality in terms of processing contained the least levels of elemental concentration. The brand is highly priced on the local market at a cost of Kshs 65 in comparison to *Jogoo* and *ugali* (Kshs 50 and Kshs 46 respectively). The relatively high concentration levels of calcium and iron in the *jogoo* brand were probably caused by other factors not related to Maize sifting processing (Table 5.11 and Figure 5.10).

Table 5.11 Results of analysis for three brands of processed Maize Flour with Fresh Maize in $\mu\text{g/g}$ after sample digestion.

| Element | Hostess (n=3) | Jogoo (n=3) | Ugali (n=3) | Raw Maize (n=3) |
|---------|----------------------|---------------------|---------------------|----------------------|
| K | 1489 \pm 299(2.0)* | 1821 \pm 163(2.1) | 2057 \pm 166(2.1) | 3613 \pm 60 (2.5) |
| Ca | 26 \pm 2(1.5) | 32 \pm 3(1.6) | 43 \pm 5(1.6) | 30.0 \pm 1 (2.0) |
| Ti | 1.7 \pm 0.2(0.5) | 2.3 \pm 0.6(0.5) | 2.9 \pm 0.5(0.5) | 2.9 \pm 0.3 (0.6) |
| Mn | 1.9 \pm 0.4(0.4) | 2.9 \pm 0.4(0.4) | 3.3 \pm 0.4(0.4) | 3.3 \pm 0.3 (0.3) |
| Fe | 19 \pm 3(0.4) | 28 \pm 6(0.4) | 39 \pm 6(0.4) | 29.0 \pm 0.3 (0.3) |
| Ni | 0.6 \pm 0.2(0.4) | 0.7 \pm 0.2(0.4) | 0.5 \pm 0.2(0.4) | 0.9 \pm 0.4 (0.3) |
| Cu | 0.9 \pm 0.1(0.4) | 1.2 \pm 0.3(0.4) | 1.0 \pm 0.1(0.4) | 1.3 \pm 0.4 (0.4) |
| Zn | 7.0 \pm 0.2(0.5) | 10 \pm 2(0.5) | 13 \pm 1(0.5) | 24 \pm 3 (0.4) |
| Rb | 1.9 \pm 0.1(0.5) | 2.4 \pm 0.7(0.5) | 2.3 \pm 0.2(0.5) | 7.3 \pm 0.3 (0.4) |

(* Limits of Detection)

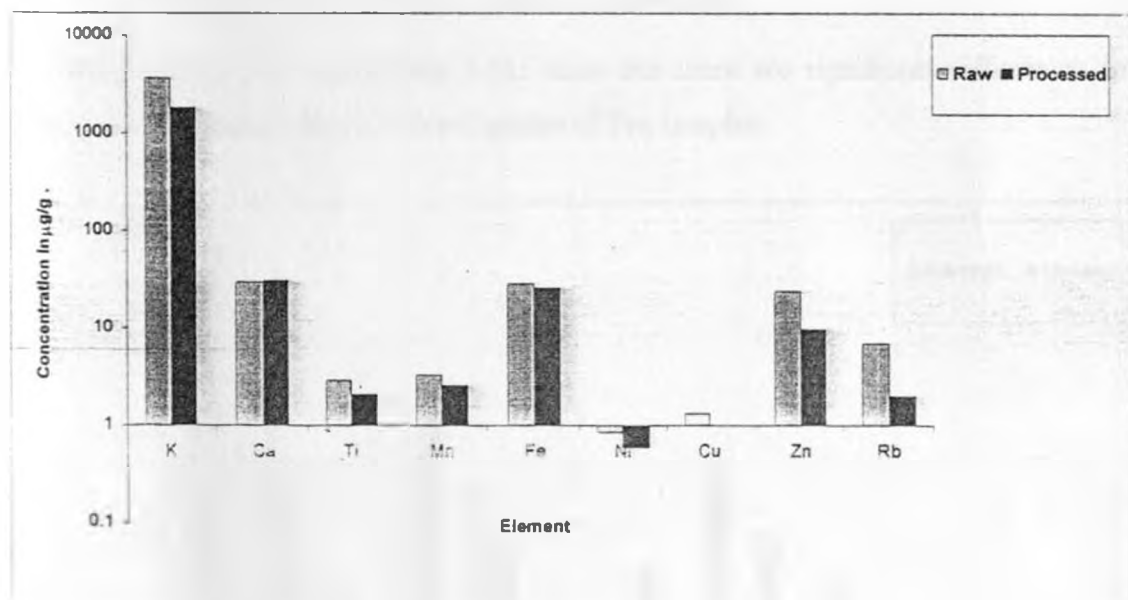


Figure 5.10 Comparison of concentrations in $\mu\text{g/g}$ for the unprocessed Maize (raw) and the mean value for processed brands (Sifted).

The sifting processing of Maize suppresses the concentration levels of potassium, zinc and rubidium by order of magnitude 50, 60 and 70% respectively.

b) Tea Leaves

Table 5.12 Concentration levels of trace elements in µg/g of instant and normal Tea brands

| Element | Normal Tea leaves ±1 s.d.(n=9) | Instant Tea ±1 s.d.(n=3) |
|---------|--------------------------------|--------------------------|
| K | 16965±3636 (9)* | 77234±1601 (20)* |
| Ca | 3367±399 (5) | 403±40 (12) |
| Ti | 30±9 (1.6) | <3.5 |
| Mn | 1060±169 (1.6) | 3007±80 (3.5) |
| Fe | 345±76 (1.6) | 83±20 (3.5) |
| Ni | 3.54±1.3 (1.6) | 8±1 (3.5) |
| Cu | 13.5±2.7 (1.6) | 55±3 (3.5) |
| Zn | 3.1±6 (1.6) | 543±15 (3.5) |
| Rb | 116±26 (1.6) | 4±1 (3.5) |
| Sr | 42±8 (1.6) | <3.5 |

(* Limits of Detection)

The results (Table 5.12 and Figure 5.11) show that there are significant differences in the elemental concentration levels of two grades of Tea samples.

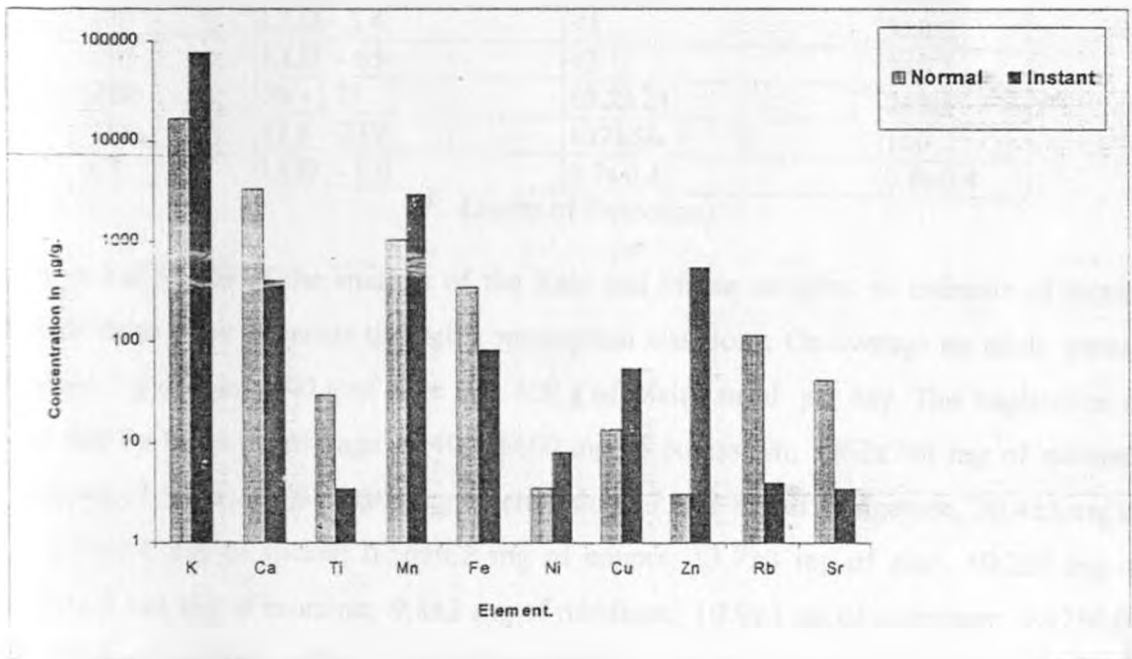


Figure 5.11 Comparison of analysis results of concentration in µg/g for normal and instant Tea.

This is probably due to the processing of the original Tea leaves to yield the different qualities of Tea. For example, in production of instant Tea, potassium, manganese, nickel, copper and zinc concentration increased by a factor of 4.6, 2.8, 2.3, 4.1 and 175 times respectively. Calcium, titanium, iron, rubidium and strontium reduced by over 8, 10, 3, 29

and 12 times respectively. Titanium was below detection limits in instant Tea. One consequence of the elevated levels of potassium concentration in the instant Tea sample was the increase in detection limits by a factor of over two.

c) Kale

The results of analysis of Kale samples are presented in Table 5.13.

Table 5.13 Concentration levels in $\mu\text{g/g}$ of elements in various Kale samples unless otherwise indicated (n=10)

| Element | Concentration range | Mean Concentration | LLD* |
|---------|---------------------|--------------------|---------------|
| K | 2.20 - 4.20% | 2.95 \pm 1% | 13 \pm 3 |
| Ca | 1.67 - 4.25% | 3.05 \pm 0.7% | 9 \pm 2 |
| Cr | 2.0 - 5.9 | 3.27 \pm 0.9 | 2 \pm 0.5 |
| Mn | 30 - 105 | 56.5 \pm 28 | 2 \pm 0.5 |
| Fe | 55 - 141 | 93.7 \pm 24 | 2 \pm 0.5 |
| Cu | 1.5 - 4.2 | 2.4 \pm 0.9 | 2 \pm 0.5 |
| Zn | 42.3 - 155 | 96.5 \pm 44 | 2 \pm 0.5 |
| Sc | LLD - 3.4 | <3 | 3 \pm 0.5 |
| Br | LLD - 65 | <3 | 3 \pm 0.5 |
| Rb | 50 - 129 | 89.2 \pm 24 | 2 \pm 0.5 |
| Sr | 31.6 - 239 | 107 \pm 56 | 1 \pm 0.2 |
| Y | LLD - 1.6 | 0.7 \pm 0.4 | 0.8 \pm 0.4 |

(* Limits of Detection)

Based on the results of the analysis of the Kale and Maize samples, an estimate of dietary intake of these trace elements through consumption was done. On average an adult person consumes 1 g of Tea, 100 g of Kale and 400 g of Maize meal per day. The implication of this is that he takes an average of 4000 \pm 600 mg of potassium; 3062 \pm 700 mg of calcium; 1.2 \pm 0.2 mg of titanium; 0.33 \pm 0.1 mg of chromium; 7.8 \pm 2 mg of manganese, 20.4 \pm 3 mg of iron; 0.24 \pm 0.1 mg of nickel; 0.66 \pm 0.2 mg of copper; 13.7 \pm 3 mg of zinc; <0.250 mg of selenium; 2.1 \pm 1 mg of bromine; 9.8 \pm 2 mg of rubidium; 10.9 \pm 3 mg of strontium; 0.07 \pm 0.04 mg of yttrium per day. What is assimilated by the various organs is a subject of further studies. From these results evidently the biggest proportions of trace element's intake are derived mainly from Kale, though the amounts indicated could be far less compared to other cereal meals. A comparison between trace element intake in Kenya common diets based on the above facts, and the UK (Hamilton and Minsk, 1972/3) showed that Kenyans consume much of manganese, rubidium, strontium and yttrium are largely due to high consumption of

Kale in their diet. Food processing mechanisms reduces the levels of some of the trace elements. Alternatively, the Britons consume more cereal based food enriched with potassium, calcium, titanium and bromine and fewer amounts of rubidium, strontium, yttrium (Figure 5.12). However, the high bromine level could be a result of either table salt or sea foods. The determined concentration levels of trace elements in raw food in Kenya are a close approximation since most people rarely add additives to their diets other than the common table salt and probably a little fat! The latter of which causes an increase bromine intake.

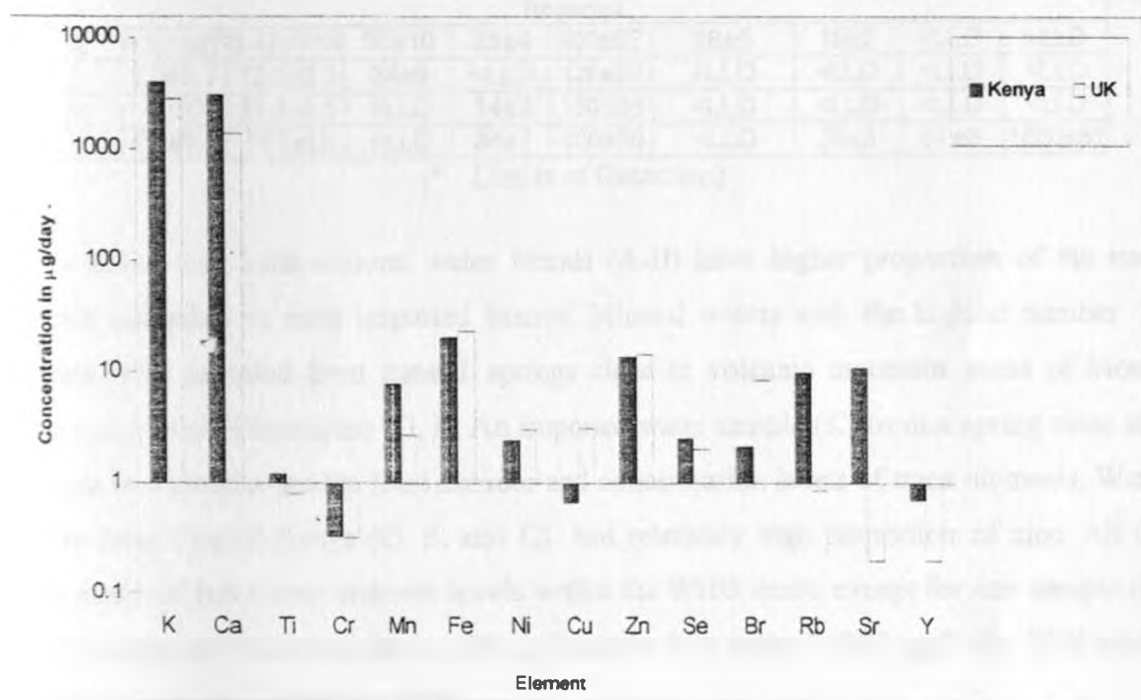


Figure 5.12 Comparison of trace element intake in mg/day for food stuff in UK (1973) and average content in common raw food in Kenya.

5.3.3 Mineral Water Samples

The results of the analysis of the water samples are presented in Table 5.14 for thirteen mineral waters: local (A-I), imported (K-N) and tap water (J).

Table 5.14 Analysis results for different water samples.

| Units | mg/ml | | µg/l | | | | | | |
|-----------------|-------------|--------------|-----------|----------|----------|----------|----------|-----------|-----------|
| Sample (LLD)* | K (0.2±0.1) | Ca (0.1±0.5) | Ti (11±2) | Mn (8±2) | Fe (8±2) | Zn (8±2) | Br (8±2) | Rb (10±2) | Sr (10±2) |
| Local | | | | | | | | | |
| A | 13.1±0.3 | 8.8±0.2 | 60±19 | 40±20 | 530±90 | 70±30 | <LLD | 26±2 | 33±6 |
| B | 11.2±0.2 | 9.8±0.2 | 49±6 | 40±16 | 520±50 | 611±10 | 223±7 | 33±4 | 70±8 |
| C | 8.2±0.1 | 7.4±0.2 | 28±5 | 23±4 | 260±50 | 1340±10 | 151±4 | 28±4 | 46±3 |
| D | 7.9±0.2 | 10.5±0.2 | <LLD | 11±4 | 31±3 | 200±50 | 107±6 | 28±4 | 40±8 |
| E | 9.7±0.2 | 11.4±0.2 | 26±6 | 35±8 | 380±50 | 20±9 | 120±10 | 33±6 | 37±3 |
| F | 2.4±0.1 | 27.3±0.5 | 34±6 | 20±7 | 420±30 | 2640±30 | <LLD | <LLD | 125±5 |
| G | 11.6±0.1 | 23.9±0.2 | 40±7 | 31±8 | 540±40 | 4730±200 | 246±10 | 40±8 | 102±6 |
| H | 12.5±0.2 | 4.7±0.1 | 40±9 | 670±6 | 320±40 | 440±30 | 14±3 | 19±2 | 16±3 |
| I | 28.8±0.5 | 23.6±0.2 | 37±4 | 35±17 | 340±40 | 33±13 | 34±3 | 20±3 | 142±6 |
| J | 6.8±0.2 | 2.2±0.1 | 26±3 | <LLD | 230±30 | 12±1 | <LLD | <LLD | <LLD |
| Imported | | | | | | | | | |
| K | 0.3±0.07 | 0.47±0.04 | 50±10 | 25±4 | 400±97 | 28±5 | 15±2 | <LLD | <LLD |
| L | 1.0±0.1 | 12.0±0.3 | 34±6 | <LLD | 125±30 | <LLD | <LLD | <LLD | <LLD |
| M | <LLD | 21.4±0.5 | <LLD | 14±3 | 150±35 | <LLD | <LLD | <LLD | <LLD |
| N | 5.6±0.9 | 131±13 | <LLD | 34±7 | 400±50 | <LLD | 35±3 | 57±8 | 1000±81 |

(* Limits of Detection)

It is observed that local mineral water brands (A-H) have higher proportion of the trace elements compared to most imported brands. Mineral waters with the highest number of elements were sampled from natural springs close to volcanic mountain areas of Mount Kenya and Mount Kilimanjaro (G, D). An imported water sample (K) from a spring close to a mountain in Australia had the least number and concentration levels of trace elements. Water samples from Central Kenya (G, F, and C) had relatively high proportion of zinc. All the waters analysed have trace element levels within the WHO limits except for one sample (H) whose manganese value was above 100 µg/l and the iron values <300 µg/l for 30 % of the total samples analysed (WHO, 1989).

Samples D (local) and N (imported) were unique in their iron and strontium content respectively. Iron was relatively low (31 µg/l) in sample D and strontium quite high in sample N as compared to the rest of the samples. Apart from some few other anomalies in concentration levels of some elements in the water samples, the general trends showed a strong correlation to the crustal rock compositions and less of the sea (Burbidge, 1957).

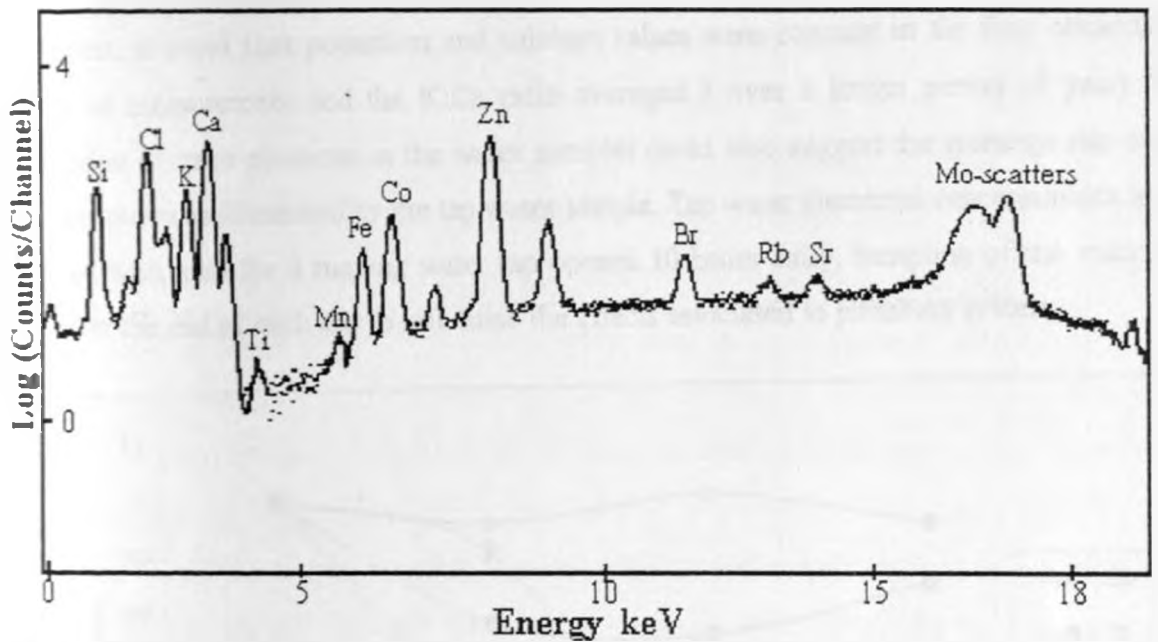


Figure 5.13 Typical spectrum of mineral water sample (G) with relatively high concentration of zinc elements. Cobalt was used as internal standard and silicon is from the sample carrier used.

In the analyses of the mineral water samples, the values for potassium and calcium, predetermined (Labeled values) for some samples, and the experimental values, agreed at 0.95 significant level. However variation of over 100% in elemental concentration are observed for some samples (K in D, M) and (Ca in G, M) as shown in table 5.15.

Table 5.15 Comparison of experimental and predetermined values of potassium (K) and calcium (Ca) in $\mu\text{g/ml}$ for some samples.

| Sample | A | D | E | G | I | M | N |
|------------------------|----------------|----------------|----------------|----------------|----------------|----------------|---------------|
| K, Experimental value | 13.1 ± 0.3 | 7.9 ± 0.2 | 9.7 ± 0.2 | 11.6 ± 0.1 | 28.9 ± 0.5 | <0.3 | 5.6 ± 0.9 |
| Predetermined value | - | 2.4 | 9.5 | - | 23 | 1 | 4.9 |
| Ca, Experimental value | 8.8 ± 0.2 | 10.5 ± 0.2 | 11.4 ± 0.2 | 24 ± 0.2 | 23.6 ± 0.2 | 21.4 ± 0.5 | 131 ± 13 |
| Predetermined value | 6.5 | 9.05 | 18 | 68 | 24 | 78 | 91 |

The experimental values of potassium were generally higher than the predetermined (label) values whereas calcium values were less in majority of the samples. The source of variation between the experimental and the predetermined values was probably caused by non uniformity in the distribution of these elements with time (seasonal) of the samples at the source. It was observed during the course of study, that the concentrations levels of the various elements contained in tap water varied with its usage or recharge (Figure 5.14). In the

analysis, it noted that potassium and calcium values were constant in the four consecutive days of measurement and the K:Ca ratio averaged 3 over a longer period (1 year). The variation of trace elements in the water samples could also suggest the recharge rate of the water source as illustrated by the tap water sample. Tap water elemental concentrations levels varied with time for a running water tap opened 10 hours daily. Sampling of the water was done at the end of each day to minimise the effects associated to plumbing system.

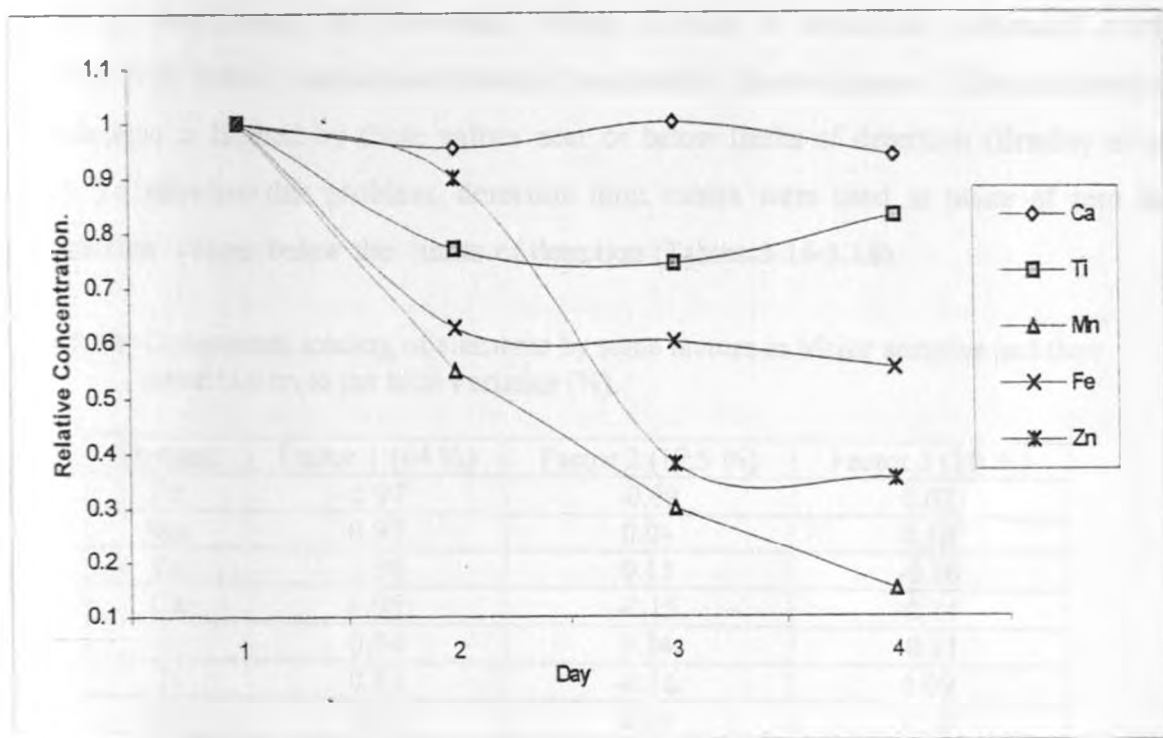


Figure 5.14 Relative concentration variation of trace elements in a running tap.

The predetermined iron values for sample A was 60 $\mu\text{g/l}$ and 200 $\mu\text{g/l}$ for sample G, while the experimental values are 530 and 540 $\mu\text{g/l}$, respectively. Manganese and zinc in the same sample (G) was given as 20 $\mu\text{g/l}$ and 200 $\mu\text{g/l}$ respectively, compared with the experimental values of 31 $\mu\text{g/l}$ and 4730 $\mu\text{g/l}$ respectively, suggesting contamination from components used during bottling, filtration or from other secondary sources like the bottle material. The duration of water storage in the bottles (containers) may have affected the water quality. Analysis of the PVC container of sample D contained the following trace elements: iron = $1.0 \pm 0.1 \mu\text{g/g}$, copper = $23 \pm 2 \mu\text{g/g}$, zinc = $10 \pm 1 \mu\text{g/g}$, lead = $8 \pm 1 \mu\text{g/g}$, based on the side of bottle originally in contact with the water sample. However, copper and lead levels in this particular water (sample D) were below the limits of detection values, 8 and 15 $\mu\text{g/l}$ respectively. This fact rules out the possibility of contamination by the PVC containers.

5.3.3 Principal Component Analysis (PCA) of Analytical Results

Principal Component Analysis was done to try and explain the contributing factors causing the difference in concentration levels in the samples (Evanston, 1989). Significant factors whose eigenvalues exceeded 10% of the total observed variance are presented below for Maize, Tea and Kale for the various elemental loading. The use of correlation matrix was adopted in determining the elemental loading because it minimises systematic errors associated with sample preparation through concentration standardization. The sensitivity of this technique is limited by those values near or below limits of detection (Bradley *et al*, (1982). To alleviate this problem, detection limit values were used in place of zero for concentration values below the limits of detection (Tables 5.16-5.18).

Table 5.16 Component loading of elements by some factors in Maize samples and their contribution to the total variance (%).

| Element | Factor 1 (64 %) | Factor 2 (17.5 %) | Factor 3 (10 %) |
|---------|-----------------|-------------------|-----------------|
| Fe | 0.97 | -0.09 | 0.02 |
| Mn | 0.97 | 0.04 | 0.18 |
| Zn | 0.96 | 0.15 | -0.16 |
| Ca | 0.95 | -0.15 | -0.14 |
| K | 0.94 | 0.14 | -0.11 |
| Ti | 0.83 | -0.36 | 0.09 |
| Rb | 0.67 | 0.58 | 0.19 |
| Cu | -0.15 | 0.8 | 0.51 |
| Ni | 0.09 | -0.64 | 0.73 |

The results showed that the first factor with high loading on the elements (iron, manganese, zinc, calcium, potassium, titanium, and rubidium) describes the inherent elements typical of the Maize flour. The second factor clustered (nickel, rubidium, copper) which probably correlates the various sub species of the Maize plants. The third factor brings those elements probably due to environmental pollution (copper and nickel).

Table 5.17 Component loading of elements by some factors in Tea samples and their contribution to the total explained variance (%).

| Element | Factor 1 (41.5 %) | Factor 2 (30 %) | Factor 3 (17 %) |
|---------|-------------------|-----------------|-----------------|
| Cu | 0.96 | -0.09 | -0.17 |
| Rb | 0.94 | 0.11 | 0.02 |
| K | 0.9 | 0.32 | -0.23 |
| Zn | 0.75 | -0.07 | 0.4 |
| Fe | 0.63 | -0.72 | 0.12 |
| Ti | 0.39 | -0.86 | 0.11 |
| Ca | 0.28 | 0.81 | 0.28 |
| Ni | 0.02 | -0.81 | 0.39 |
| Mn | 0.33 | 0.51 | 0.75 |
| Sr | 0.49 | 0.11 | -0.81 |

Tea leaves are characterised by the elements (copper, rubidium, potassium, zinc, iron, and strontium), attributed to factor one. Factor two, is probably the environmental condition affecting the availability of the elements (calcium, manganese, titanium, nickel, iron) to the Tea plant. The third factor involving the elements (manganese, strontium) is probably due to the processing mechanism used in Tea leaves preparation.

Table 5.18 Component loading of elements with significant factors in Kale sample and the factor contribution to the total explained variance (%).

| Element | Factor 1 (44.8 %) | Factor 2 (20.2 %) | Factor 3 (17.3 %) |
|---------|-------------------|-------------------|-------------------|
| Y | 0.84 | -0.18 | 0.26 |
| Mn | 0.84 | 0.16 | 0.45 |
| Rb | 0.83 | 0.44 | 0.04 |
| Zn | 0.80 | 0.15 | 0.49 |
| Cr | -0.62 | -0.72 | -0.13 |
| K | 0.59 | -0.16 | -0.41 |
| Ca | -0.59 | 0.43 | 0.51 |
| Sr | -0.56 | 0.77 | 0.01 |
| Cu | 0.54 | 0.26 | -0.78 |
| Br | -0.51 | 0.72 | -0.25 |
| Fe | 0.48 | 0.21 | -0.53 |

The factors correlating the elements of high loading in Kale are not easily explained. The first factor is probably a mixed factor of the inherent trace element's characteristic of the Kale leaves (yttrium, manganese, rubidium, zinc, potassium, copper, and iron) and the environmental conditions affecting them (chromium, strontium, and bromine). A likely explanation was the possibility that the Kale leaves were contaminated by soil on which they were grown. This contamination was not completely removed by the initial rinsing in double

distilled water before the samples were analysed. The second factor clustering (strontium, bromine and chromium) was probably an environmental factor with chromium being introduced as a result of environmental pollution. The third factor seemed to cluster those elements that correlate the different sub-species of Kale.

The results given by the factor analysis showed that Kale, Maize and Tea, have three factors exceeding 10 % which explained over 90 % of the total concentration variance in the elemental concentration. Unlike the other two samples, the Kale had a negative correlation in the first factor, indicating that the inherent factor for the trace elemental concentration profile in Kale was compounded by another factor.

Principal Component Analysis was applied to explain the factors contributing to the observed elemental concentration profile in the water samples. The results showed that four significant factors that could explain more than 10% of the total sample variances (Table 5.19).

Table 5.19 Component loading of elements with significant factors in water samples.

| Element | Factor 1 (31.4%) | Factor 2 (27.3%) | Factor 3 (14.8%) | Factor 4 (11%) |
|---------|---------------------|---------------------|---------------------|-------------------|
| Rb | 0.88 | 0.21 | 0.07 | -0.30. |
| Sr | 0.88 | -0.37 | 0.18 | 0.21 |
| Ca | 0.86 | 0.42 | 0.11 | 0.22 |
| Ti | -0.31 | 0.78 | 0.28 | 0.58 |
| Fe | 0.40. | 0.72 | 0.17 | 0.49 |
| Br | 0.39 | 0.61 | -0.48 | -0.40. |
| Zn | 0.24 | 0.58 | -0.50. | 0.14 |
| Mn | -0.14 | 0.15 | 0.67 | -0.18 |
| K | 0.19 | 0.49 | 0.50. | -0.46 |

The component loading of the first factor reflects the chemistry of these three elements (rubidium, strontium and calcium) showing that hydrochemistry elements play an important role in trace element distribution in water samples, the second factor reflects the nature of the crustal composition at the source of the sample (soil composition and pH) based on the cluster of element's titanium, iron, bromine and zinc. The third factor that clustered manganese is probably the water sample pH factor. These three factors contributed close to 75 % of the total variance of the concentration results obtained for the trace element content of water.

The detection limits of elements in water samples just like the other analysed samples, were found to be quite sensitive to the presence of low Z matrices, mainly chlorine, phosphorus, potassium and calcium. For the samples with high concentrations of these elements, Tea and Kale samples, the limits of detection are higher than those of lower concentrations, Rye Flour, 'Rice unpolished', Maize samples. For water samples with high concentrations of some of these elements (G, I, N), had higher lower limit of detection than those with relatively lower concentrations, (K and L). Other factors which affected the lower limit of detection were noted as uncontrolled spreading and sample volume spiked. Lower limit of detection was noted to deteriorate with the number of times a sample carrier is used. This was noted to affect mainly elements in the energy region >7.0 KeV. For example, lower limit of detection of strontium was initially $9 \mu\text{g/l}$, but increased to almost $13 \mu\text{g/l}$ on the 25th re-use of the sample carrier. This may be attributed to the surface etching of the carrier surface during cleaning and the consequent loss of reflectivity.

CHAPTER SIX

CONCLUSION AND RECOMMENDATIONS

6.1 Conclusion

- ◆ Relatively clean sample carriers could be achieved using a simple cleaning procedure.
- ◆ One of the major problem of sample homogeneity in TXRF analysis was improved by drying the sample carriers at 60 °C for 10 hours. This enabled the samples to spread on the carrier to about 6 mm in diameter.
- ◆ Water samples from different places have different elemental composition depending on the parent crustal rocks, but may also be modified by the geochemistry of the source, preparation or storage.
- ◆ Most of the Kenyan mineral water samples contained relatively higher levels of potassium, iron, zinc, bromine, rubidium and strontium compared to the imported brands.
- ◆ TXRF measurements indicate that Fe concentration levels in 50 % of the imported and 80 % of the local water samples exceed the WHO limits (<300 µg/l).
- ◆ Toxic elements(Pb, Hg) levels were below detection limits (15 µg/l) in all the analysed samples.
- ◆ Volcanic water sources seem to have high elemental composition.
- ◆ Trace element intake in Kenyan's major diet is enhanced by Kale consumption (*Brassica oleracea*), especially for the elements strontium (107±59 µg/g) and rubidium (89±25 µg/g). Tea leaves (*Camelia sinensis*) contribute substantial amounts of manganese (1060±169 µg/g) and rubidium (116±26 µg/g) whereas Maize meal (*Zea mays*) contributes high proportions of iron (27±9 µg/g).

- ◆ Food processing mechanism affects the trace element levels.
- ◆ Principal Component Analysis of the water results revealed three significant factors with the highest loading clustering rubidium, strontium, calcium in the first eigenvalue; titanium, iron, bromine, zinc, in the second; zinc, manganese, potassium in the third.
- ◆ Principal Component Analyses of the ten Maize samples showed that, 64% of the observed total elemental concentration variance, was explained by a single factor (elements of highest loading (iron, manganese, calcium, titanium and rubidium). For Kale and Tea samples, the most significant factor explained only 45 % (elements of highest loading copper, rubidium, potassium, zinc and iron) and 42 % (elements of highest positive loading yttrium, manganese, rubidium and zinc) respectively. For the case of the water samples, results revealed three significant factors with the highest component loading clustering of rubidium, strontium, calcium in the first eigenvalue (31.4 %); titanium, iron, bromine, zinc, in the second (27.3 %); zinc, manganese, potassium in the third (14.8 %).
- ◆ There is no significant difference between certified values and the experimental values for most elements analysed.

6.2 Recommendations

- ◆ Proposed improvement on sensitivity of the TXRF technique:
 - Use of evacuated sample-detector chamber
 - A finer beam x-ray tube for increased flux intensity to the sample.
 - Ultra trace element studies require efficient sample preparation by preconcentration procedures.
 - Low angles of incident radiation give better sensitivities for samples containing low concentration of low atomic number elements (dark matrix).

- ◆ Because of the interactive nature of elements both in the body, multi-disciplinary elemental studies are essential, to provide data on the patterns and causal relationship between trace element intake and health-disease.

- ◆ The analysis has confirmed that processing alters trace element content of food. Thus more research is needed to determine the extent of alteration in all types of processed food and the ultimate consequence to human health.

- ◆ The introduction of new varieties of plants, the use of agricultural chemicals and other new techniques designed to increase food production are likely to affect the absorption of trace elements by the basic food crops. A further study is therefore recommended.

- ◆ TXRF is a reliable tool for water quality control quality and assessment and therefore useful to the authorities enforcing the maximum acceptable levels of trace elements in drinking water.

References:

- Aiginger, H. and Wobrauschek, P., A Method for Quantitative XRF Analysis in the Nanogram Region, *Nuclear Instr. and Meth.*, **114**, 157, (1974).
- Atsuo, I., Yoshinaga, A., Sakurai, K. and Ghoshi, Y., Sr Excited XRF Analysis using Total Reflection of X-rays, *Anal. Chem.*, **58**, 394 (1986).
- Bertin E. P., *Introduction to X-ray Spectrometry*, NY, (1973).
- Bertin, E. P., *Principles and Practice of X-ray Spectrometric Analysis*, Plenum Press, (1975).
- Bohlen, A. V., Klockenkamper, R., Tolg, G. and Wiecken, B., Microtome Sections of Biomaterials for Trace Analyses by TXRF, *Fresenius' Z. Anal. Chem.* **331**, 454, (1988).
- Bohlen, A. V., Eller, R., Klockenkamper, R., and Tolg, G., Micro-analysis of Dissolved Samples by Total Reflection X-ray Fluorescence Spectrometry, *Anal. Chem.*, **59**, 2551, (1987).
- Bohlen, A. V., Klockenkamper, R., Otto, H., Tolg, G. and Wiecken, B., Qualitative Survey Analysis of Thin Layers of Tissue Samples - Heavy Metal Traces in Human Lung Tissue, *Int. Arch. Occup Environ Health*, **59**, 403 (1987).
- Bradley, A. R., Hopke, K. P., Dattner, S. L., Jenks, J. M., (1982), The use of Principal Component Factor Analysis to Interpret Particulate Compositional Data Sets. *Journal of Air Pollution Control*, Vol. 32. No. 6.
- Burbidge, E. M., Burbidge, G. R., Fowler, W. A., Hoyle, F., Synthesis of Elements in Stars, *Rev. Mod. Phys.* **21**, 625, (1957).
- Canberra Si(Li) Detector Operation Manual, (1994).
- Compton, A., *Phil. Mag.*, **45**, 1121, (1923).
- Davies, N. T., Nightingale, R., The Effects of Phylate on Intestinal Absorption and Secretion of Zinc and Whole Body Retention of Zinc, Copper, Iron and Manganese by in Rats. *Br. J. Nutr.* **34**, 75-85, (1975).
- Evanston, I. L., *Systat*, The System for Statistics for the PC, Systat Inc. (1989).
- Gerwinski, W. and Göetz, D., Multielemental Analysis of Standard Reference Materials with Total Reflection X-ray Fluorescence, *Fresenius' Z. Anal. Chem.*, **327**, 690, (1987).
- Hambidge, K. M., Chromium Nutrition in Man, *Am. J. Clin. Nutr.* **27**, 505, (1974).
- Hamilton, E. T., The Chemical Elements and Human Morbidity-Water, Air and Places-a

- Study of Natural Variability, *Sci. Total Environ.* 3 (1974).
- Hamilton, E. I., Minsk, M. J., Abundance of the Chemical Element in Man's Diet and Possible Relations with Environmental Factors, *Sci. Total Environ.* 1, 375, (1972/3)
- Holynska, B., University of Mining & Metallurgy., Krakow, *Pers. com.*, (1996).
- Holynska, B., Sampling and Sample Preparation in EDXRS, *X-ray Spect.*, Vol. 22, 192-198, (1993).
- Iyengar G. V., Sansoni, B., Elemental Analysis of Biological Materials, in Technical Report series, No 197. IAEA, Vienna. (1980), Chap. 6, 73.
- Jackella, D. T., Knap, A. H. and Church, T.M., *J. Geophy. Res.*, 88, 123, (1984).
- Johns, H. E., *The Physics of Radiology*, Charles Thomas, 4th Edition, (1953).
- Junge, C. E., *Air Chem. and Radioactivity*, Academic Press, NY, (1963).
- Kinyua, A. M., MSc Thesis, University of Nairobi, (1982).
- Klockenkamper, K. and Bohlen, A. V., Determination of the Critical Thickness and the Sensitivity for Thin Film Analysis by TXRF Spectrometry, *Spectrochim. Acta.*, Vol. 446, No 5, 461-469, (1989).
- Knoll, G. F., *Radiation Detection and Measurements*, John Wiley & Sons, Inc., (1979).
- Knoth, J. and Schwenke, H., An X-ray fluorescence Spectrometer with Totally Reflecting Sample Support for Trace Analysis at the ppb level, *Fresenius' Z. Anal. Chem.* 291, 200, (1978).
- Knoth, J., Schwenke, H. and Weisbrod, U., Total Reflection X-ray Fluorescence Spectrometry for Surface Analysis, *Spectrochim. Acta.*, 44B, 477, (1989).
- Kregsamer, P. K., Manual for QXAS, *Quantitative X-ray Analysis System* (Version 3.2), IAEA, (1995).
- Leland, D. J., Bilbrey, D. B., Leyden, D. E., Wobrauschek, P., Aiginger, H. and Puxbaum, H., Analysis of Aerosols using Total Reflection X-ray, *Spectro. Anal. Chem.*, 59, 1911, (1987).
- Magil, P. L., Holden, F. R. and Ackley, C., *Air pollution Handbook*, MCGraw Hill, NY, (1956).
- Marquardt, D. W., Non Linear Least Square Algorithm, *J. Sol. Ind. Appl. Math.*, 11, 431, (1963).
- Masironi, R., Musch, A. T., Crawford, M. D., Hamilton, E. F., Geochemistry Environment, Trace Elements and Cardiovascular Diseases. Bull World Health Organ. 47, 139, (1972).
- Mentasti, E., Nicoletti, A., Parta, V. and Sarzanini, C., *Analyst*, 114, 1113, (1989).

- Mertz, W., *Biological Trace Element Research*, 1, 259-270, 1979.
- Michaelis, W., Studies of the Heavy Metal Transport in Tidal Rivers, *Proc. Int. Conf. on Heavy Metals in the Environment*, Heidelberg, F.R.G., Vol. II, 972, GKSS 83/E/43, 6-9 Sept 1983.
- Michaelis, W. and Prange, A., Trace Analysis of Geological and Environmental Samples by Total Reflection X-ray Spectrometry, *Nuclear Geophysics*, 2, 231 (1988).
- Moens, L., Devos, W., Klockenkamper, R. and Bohlen, A.V., Application of TXRF for ultra Micro Analysis of Artists Pigments, *J. Trace and Microprobe Techniques*, 13(2), 119, 1985.
- Muia, L.M., Ph.D Thesis, University of Antwerp, (1991).
- Nakana, Y., Fukamachi, F. and Hayakowa, Jpn. J. Appl. Phys., 17, 329, (1978).
- Ninomiya, T., Nomura, S., Taniguchi, K. and Ikeda, S., *Adv. X-ray Anal.*, 32, 197, (1989).
- Numberg, H. W., Valenta, P. and Nguyen, V. D., In Deposition of Atmospheric Pollutants, Georgil, Pan Krath, H. W., *J. Eds.* 143-157, (1982).
- Ojeda, N., Greaves, E. D., Alverado, J. and Sajo Bolns, L., Determination of V, Fe, Ni, S in Petroleum Crude Oil by Total Reflection X-ray Fluorescence, *Spectrochim. Acta.*, 48B, 223-229, (1993).
- Parratt, L., Surface Studies of Solids by Total Reflection of X-rays, *Phys. Rev.*, 95, 359, (1954).
- Pooreboom, J. W. C., General Aspects of Trace elements and Health, *The Science of the Total Environment*, 42, 1-27, (1985)
- Pelpelnik, R., Erbslöh, B. Michaelis, W. and Prange, A. Determination of Trace Elements in River Water using Total Reflection X-ray Fluorescence, *Spectrochim. Acta.* 48B 207-215, (1993).
- Pelpelnik, R., Erbslöh, B., Michaelis, W. and Prange, A., Determination of Trace Element Deposition in a Forest Ecosystem using Total Reflection X-ray Fluorescence, *Spectrochim. Acta.*, 48B, 223-229, (1993).
- Pinta, M., *Modern Methods for Trace Element Analysis*, Ann Arbor Science Publishers, Inc. New York. (1978).
- Prange, A., Total Reflection X-ray Spectrometry: Methods and Applications, *Spectrochim. Acta.*, Vol. 44B, No 5, 427-452, (1989).
- Prange, A. and Kremling, K., Distribution of Dissolved Molybdenum, Uranium and Vanadium in Baltic Sea Waters, *Mar. Chem.*, 16, 259. (1985).

074938/2000

Prange, A., Böddeker, H. and Kramer, K., Determination of Trace Elements in River Water using Total-Reflection X-ray Fluorescence, *Spectrochim. Acta.*, **48B**, 207-215, (1993).

Prange, A., Knoth, J., Stöbel, R. P., Boddeker, H. and Kramer, K., Determination of Trace Elements in the Water cycle by Total Reflection X-ray Fluorescence Spectrometry, *Anal. Chim. Acta.*, **195**, 275, (1985).

Prange, A., Knöchel, A. and Michaelis, W., Multi-elemental Determination of Dissolved Heavy Metal Traces in Sea Water by Total Reflection X-ray Fluorescence Spectrometry Analysis, *Chim. Acta.* **172**, 79-100, (1985).

Purves, D., *Trace Element Contamination of Environment*, Elsevier Sc. Pub. Company, (1977).

Sansoni, B., and Iyengar, G. V., Sampling and Sample Preparation Methods for the Analysis of Trace Elements in Biological materials, Report, May 1978, KFA Julich, FRG, (1978).

Sansoni, B., and Iyengar, G. V., In *Elemental Analysis of Biological Materials*, Chapter 5, (IAEA Technical report, no 197), IAEA, Vienna, (1980).

Schneider, B., and Weiler, K., A Quick Grain Size Correction Procedure for Trace Metal Contents of Sediments, *Env. Techn. Lett* **5**, 245, (1984).

Schwenke, H. and Knoth, J., A Highly Sensitive Energy-dispersive X-ray Spectrometer with Multiple Total Reflection of the Excitation Beam, *Nucl. Instrum. and Meth.*, **193**, 239, (1982).

Schwenke, H. and Knoth, J., *Hand Book on X-ray Spectrometry*, Merce! Dekker, New York, (1991).

Smits, J., Nelissen, K. and Van Grieken, R., *Anal. Chim. Acta.* **11**, 215, (1979).

Stöbel, R. B. and Prange, A., Determination of Trace elements in Rainwater by Total Reflection X-ray Fluorescence, *Anal. Chem.*, **57**, 2880, (1985).

Stöbel, R. B. and Prange, A., Studies on the Atmospheric Heavy Metal Transport into the German Bight, *Int. Conf. Heavy Metals in the Environment*, Athens, Greece, Vol. 1, p 203, Sept. (1985).

Streli, C., Aiginger, H. and Wobrauschek, P., Total Reflection X-ray Fluorescence Analysis of Low-Z elements, *Spectrochim. Acta.* **44B**, 491, (1989).

Streli, C., Aiginger, H. and Wobrauschek, P., Light Element Analysis with a New Spectrometer for Total Reflection X-ray Fluorescence, *Spectrochim Acta.* **48B**, 163-170, (1993).

- The National Research Council, Geochemistry and the Environment, Vol. II: The Relationship of Selected Trace Elements to Health and Diseases, National Academy of Sciences, Washington (1977).
- Tölg, G., Extreme Trace Element Analysis of Elements: Method and Problems of Sample Treatment, Separation and Enrichment, *Talanta* 19, 1489 (1972).
- Van Espen, P., Nullens, H. and Adams, F., A Computer Analysis of X-ray Fluorescence Spectra, *Nucl. Instru. Methods*, 142, 243, (1977).
- Van Espen, P., Nullens, H. and Adams, F., Linear and Non Linear Peak Fitting in Energy Dispersive X-ray Fluorescence, *X-ray Spectrometry*, 8, No 3, 103, (1979).
- Williams, K. L., *An Introduction to X-ray Spectrometry*, Allen and Unwin. London (1987).
- World Health Organization (WHO) Annual Report, (1989).
- Wobrauschek, P., *Adjustment and Working Instruction for LAEA Reflection Attachment. Manual*, (1989).
- Wobrauschek, P., Total Reflection X-ray Fluorescence Analysis with Polarized Radiation, *J. Trace and Microprobe Techniques*, 13 (2) 83-96, (1995).
- Wobrauschek P. and Ainginger, H., *Spectrochim. Acta.*, Part B, 35, 607, (1980).
- Wobrauschek, P. and Ainginger, H., *Adv. X-ray Anal.*, 28, 1, (1985).
- Wobrauschek, P. and Ainginger, H., Total Reflection X-ray Fluorescence Spectrometric Determination of Elements in Nanogram Amounts, *Anal. Chem.*, 47, 852. (1975).
- Wobrauschek, P., Kregsamer, P., Strelj, C. Ainginger, H., Instrumental Development in Total Reflection X-ray Fluorescence Analysis for K-lines from Oxygen to Rare Earth Elements, *X-ray Spectrometry*, Vol. 20. 23-28, (1991).
- Yoneda Y. and Horiuchi, T., Optical Flats for use in X-ray Spectrochemical Microanalysis, *Rev. Sci. Inst.* 42, 1069, (1971).